Comparing image processing pipelines for brain MRI data and examining default mode and executive control network white matter correlates of executive function in multiple sclerosis

by

Salina Sultana Pirzada

A Thesis submitted to the Faculty of Graduate Studies of

The University of Manitoba

In partial fulfillment of the requirements of the degree of

MASTER OF SCIENCE

Department of Physiology and Pathophysiology

Max Rady College of Medicine

Rady Faculty of Health Sciences

University of Manitoba

Winnipeg, MB

Abstract

Background: Multiple Sclerosis is a neurodegenerative disease characterized by demyelinated lesions and axonal loss in white matter regions of the brain. Spatially normalizing brain MRI data to a template is commonly performed to better facilitate comparisons between individuals or groups. Due to the presence of MS-related brain pathologies, spatial normalization methods can be compromised. This study therefore systematically compared five commonly used spatial normalizations for brain MRI including linear (affine), nonlinear MRIStudio (LDDMM), FSL (FNIRT), ANTs (SyN) and SPM (CAT12) algorithms to evaluate their performance in the presence of MS-related pathologies. After identifying an optimal spatial normalization method, this study then used pre-existing knowledge on the relationships between cognitive performance and resting-state functional connectivity in distributed large-scale brain networks to look at cognition, executive function and white matter structural connectivity. This would build on the previous findings in this study by using the optimal method to acquire FA and MD maps to use in conjunction with recently released functionally-defined white matter atlases to investigate relationships between executive function and microstructure throughout the default mode network and executive control network white matter.

Methods: Using a cohort of 20 participants with MS from an ongoing cohort study and 1 healthy control participant, we lesion-filled each participant's T1-weighted brain image to the Montreal Neurological Institute template using 5 normalization approaches for a real and simulated lesion dataset (total of 400 spatial normalizations). Inter-subject variability was quantified using both mutual information and coefficient of variation and normalization lesion volumes were evaluated using paired sample t-tests. Using SPM CAT12, we used diffusion tensor imaging metrics, FA and MD from 103 participants to extract values from DMN and ECN regions via the UManitoba-

Functionally-Defined Human White Matter Atlases. Executive function was assessed using the Delis-Kaplan Executive Function System Color-word Interference Test. One-tailed Spearman correlations assessed relations between DMN and ECN white matter microstructure and individual differences in executive function correcting for age, sex and WTAR scores.

Results: SPM CAT12 with lesion filling is the most robust method for spatially normalizing MS brain imaging data, as demonstrated in Coefficient of Variation maps, that make clear that SPM CAT12 resulted in the lowest average COV value (SPM: 9.6 and 21.4 for FSL). Using SPM CAT12, this study found executive function scores to be significantly correlated with individual differences in white matter MD measurements obtained from both the DMN (rho = 0.194; 96% CI = 0.0031 to 0.0347; p = 0.027) and the ECN (rho= 0.192; 95% = 0.029 to 0.345; p= 0.029), but not those obtained from global white matter (rho = 0.106; 95% CI = -0.059 to 0.0266; p = 0.147) after correcting for age, sex and WTAR.

Conclusion: Together, this thesis worked to: 1) compare spatial normalization methods on brain MRI data in the presence of MS lesions using real and simulated data to identify an optimal approach for comparing quantitative structural imaging metrics across participants, and 2) use this robust spatial normalization method to investigate the relationships between EF and microstructure throughout the DMN and ECN WM using recently released functionally-defined WM atlases. Together, these findings have expanded our understanding of best-practices in MRI data analysis and the variability in cognitive functioning among persons with MS.

Acknowledgements

I would like to thank many people who were integral in helping me achieve this degree.

Dr. Chase Figley: I am deeply indebted to you for the time and trust you put in me. You were not only my P.I., but my mentor, role model and friend. At pivotal moments during this journey, you shared with me your wisdom - for which I am forever grateful. Your ability to teach complex concepts in an enjoyable, friendly and exciting way is what made me discover my passion for neuroscience, and specifically neuroimaging. I was very fortunate to have trained under you, and will carry forward everything you have taught me. Your generosity, kindness and encouragement will stay with me forever – as this end is only the beginning of a new chapter.

Dr. Md Nasir Uddin: thank you for teaching me a lot of what I know about MR imaging. From teaching me the basics of MRI physics till more advanced topics as time went by; your continued patience and encouragement is something I am truly grateful for.

Teresa Figley: thank you for always helping me stay grounded and balanced when major deadlines approached. Your constant reminder to reflect on what research really is, and why I am pursuing it, helped shape me into a balanced neuroscientist.

My committee members – Dr. Kornelsen and Dr. Marrie: Thank you for guiding, advising and always encouraging me to be my best self throughout my journey. Without your continuous support and mentorship, I would not have achieved this degree.

To my neuroimaging pal Tiffany: You were the most supportive friend I could have asked for, and someone that I have made some of my most cherished memories in graduate school with. Thanks for being such a great friend and for cheering me on in every endeavor.

To my dearest husband Shan Pirzada; words fail to express my gratitude for your love and support on this journey. You are my rock – my greatest motivation and strength. I thank and love you with every nerve in my body, and cannot wait to see what adventures our life together has in store for us. Thank you for your love, inspiration, encouragement and limitless motivation.

I would like to thank my parents, Masood and Alia Khan: thank you for giving me strong roots that kept me grounded and strong wings that allowed me to soar at will. Thank you for every sacrifice you made in life for the betterment of our family. I am forever indebted to you for the love and support you have shown me, and hope to continue to make you proud.

Thank you to my siblings – Sophia and Zeshan. The bond I share with you remains among my greatest achievements. You both have been there for me through thick and thin, and I cannot thank you enough. You are my role models and I hope to be half the person you both are.

Thank you to my new parents – Kokeb and Munir Pirzada. The unconditional love and support I have received since the day I moved to Winnipeg cannot be put into words. You both are nothing short of my parents, and I love you both with all my heart.

To my new siblings, Yelman, Tamana, Hasan, Hafsa and Iman – despite being miles apart at times, we continue to be there for one another and support each other's dreams and ambitions, and I thank you for that. I am grateful for the closeness we share, as I truly believe a strong family unit is the foundation to true happiness and success.

Contributions of Authors on Manuscript

Drs. Chase Figley and Md Nasir Uddin as a part of the CCOMS Study helped acquire this data at the National Research Council of Canada in Winnipeg, Manitoba. Drs. Chase Figley, Jennifer Kornelsen and Dr. Ruth Ann Marrie contributed to the revision of the submitted manuscript.

Salina S. Pirzada preprocessed and analyzed the data, wrote the manuscript, and created the tables and figures (figures with the assistance of Teresa Figley and Dr. Md Nasir Uddin).

The Investigators of the Comorbidity, Cognition and Multiple Sclerosis (CCOMS) Study Group include:

Ruth Ann Marrie, MD, PhD (University of Manitoba, Principal Investigator);

John D. Fisk, PhD (Dalhousie University, Co-Principal Investigator);

James Bolton, MD (University of Manitoba, Co-Investigator);

Chase R. Figley, PhD (University of Manitoba, Co-Investigator);

Lesley Graff, PhD (University of Manitoba, Co-Investigator);

Jennifer Kornelsen, PhD (University of Manitoba, Co-Investigator);

James J. Marriott, MD (University of Manitoba, Co-Investigator);

Erin Mazerolle, PhD (University of Calgary, Co-Investigator);

Ronak Patel, PhD (University of Manitoba, Co-Investigator);

Teresa D. Figley, MSc (University of Manitoba, Research Coordinator);

Carl A. Helmick, BCS (Dalhousie University, MRI Data Analyst);

Md Nasir Uddin, PhD (University of Manitoba, MRI Physicist and Data Analyst);

Charles N. Bernstein, MD (University of Manitoba, Collaborator)

Table of Contents

List of Figures

List of Tables

Chapter 4 Tables:

List of Abbreviations

MRI: Magnetic Resonance Imaging

MS: Multiple Sclerosis

3D: Three-dimensional

T1w: T1-weighted

T2w: T2-weighted

FLAIR: Fluid Attenuated Inversion Recovery

T2-FLAIR: T2-Weighted Fluid Attenuated Inversion Recovery

MPRAGE: Magnetization prepared rapid acquisition gradient echo

HARDI: High Angular Resolution Diffusion Imaging

TR: Repetition Time

TE: Echo Time

TI: Inversion Time

BW: Band Width

ESP: Echo Spacing

TA: Acquisition Time

FOV: Field of View

MB-EPI: Multi-Band Echo Planar Imaging

AT: Anterior-Posterior

PA: Posterior-Anterior

ACID: Artifact Correction in Diffusion MRI

HySCo: Hyperelastic Susceptibility Artifact Correction

COVIPER: Correction for Vibrations in Diffusion Imaging using Phase-Encoding Reversal

DTI: Diffusion tensor imaging

FA: Fractional Anisotropy

MD: Mean Diffusivity

MWI: Myelin Water Imaging

Q-TIPS: Quantitative Tract Integrity Profiles

MTI: Magnetization transfer imaging

VBM: Voxel-based morphometry

WM: White matter

NAWM: Normal appearing white matter

ROI: Region of Interest

GM: Grey Matter

M: Net Magnetization Vector

DARTEL: Diffeomorphic Anatomical Registration Through Exponentiated Lie Algebra

BET: Brain Extraction Tool

LST: Lesion Segmentation Toolbox

LGA: lesion growth algorithm

DIS: Dissemination in Space

DIT: Dissemination in Time

Non-LF: Non-lesion-filled

LF: Lesion-filled

CSF: Cerebrospinal Fluid

NMI: Normalized Mutual Information

MNI: Montreal Neurological Institute

MRIStudio (LDDMM): (Large deformation diffeomorphic metric mapping)

FSL (FLIRT): (Linear Image Registration Tool)

FSL (FNIRT): (Nonlinear Image Registration Tool)

ANTs (SyN): Advanced Normalization Tools (Symmetric Normalization algorithm)

SPM (CAT12): Statistical Parametric Mapping (Computational Anatomy Toolbox)

SC: Structural Connectivity

FC: Functional Connectivity

JHU: Johns Hopkins University

HLA: Human Leukocyte Antigen

CTLA: Cytoxic T Lymphocyte Antigen

ICAM: Intracellular Adhesion Molecule

MSFC: Multiple Sclerosis Functional Composite

EDSS: Expanded Disability Status Scale

DKEFS: Delis-Kaplan Executive Function System

DMN: Default Mode Network

dDMN: Dorsal Default Mode Network

vDMN: Ventral Default Mode Network

ECN: Executive Control Network

1ECN: Left Executive Control Network

rECN: Right Executive Control Network

DKEFS CWIT: Delis-Kaplan Executive Function System Color-Word Interference Test

DKEFS TMT: Delis-Kaplan Executive Function System Trail Making Test

CN: Color Naming

WR: Word Reading

EF: Executive Function

WTAR: Wechsler Test of Adult Reading

CVLT II: California Verbal Learning Test

PASAT: Paced Auditory Serial Addition Test

MET: Multiple Errands Test

WCST: Wisconsin Card Sorting Test

B-REB: Biomedical Research Ethics Board

COV: Coefficient of variation

DSC: Dice similarity coefficient

MI: Mutual information

CCOMS: Comorbidity, Cognition and Multiple Sclerosis

HSCF: The Winnipeg Health Sciences Centre Foundation

NSERC: Natural Sciences and Engineering Research Council of Canada

Chapter 1: Introduction

1.1 Etiology and Prevalence of MS

Multiple sclerosis (MS) is a chronic neurodegenerative disease of the central nervous system (CNS)[1]. It is the most common disabling neurological disease in young adults, with a typical onset between 20 to 40 years of age, affecting twice as many females as males[2,3]. In terms of prevalence, currently MS affects over 2.5 million people worldwide with roughly 290 cases per 100,000 Canadians, with the prairie provinces – particularly Manitoba having amongst the highest rates of MS in the world[3,4]. Although there is no known cause for MS, the disease itself has a complex etiology, with both genetic and environmental components contributing to the onset of the disease, with the risks being associated with exposure to environmental factors in genetically susceptible individuals[3]. In fact, studies suggest that Caucasians are the most affected, with a much lower prevalence among Japanese, Chinese, American Indians and individuals of African descent[3]. Because of this, many studies have suggested that environmental conditions in regions with higher latitudes in both hemispheres may foster environmental conditions optimal for developing MS.

Much of the literature regarding prevalence, is tied to migration and MS. These migration studies reported that individuals growing up in high-prevalence areas remain at a higher risk for developing MS, even after moving to a low-risk region. Interestingly however, migration from a low-risk to a high-risk region during childhood seems to increase the risk of developing MS[1]. Considerable evidence has also led to the popular belief that these high-risk areas which happen to be situated in higher latitude regions worldwide, generate a lower duration and intensity of sunlight, creating environments that trigger low vitamin D levels - which is considered by some to be an environmental risk factor for MS. In fact, one record-linkage study found skin cancer mortality rates to be 50% less among MS patients, potentially supporting the correlation between

reduced sunlight exposure and MS[5]. This then begs the question of what the effects of other environmental risk factors have on those who are genetically susceptible? One such study looked at the association between sun exposure in childhood and MS risk among 81 monozygotic twins, and found that twins with MS systematically reported lower levels of sun exposure, therefore supporting the possibility that reduced early sun exposure prompts the onset of MS[6].

Moreover, one putative factor with a strong biologic plausibility is obesity, as it has been shown to increase the risk of developing MS. In fact, some studies have found obesity, coupled with an early age of sexual maturity to be associated with the onset of MS - with the pediatric population of MS in particular being affected the most. One study in particular comprised of 1571 cases and 3371 controls reported a two-fold increase in the risk for MS patients with a BMI exceeding 27 kg/m^2. This pattern of association was the same for both men and women[7]. Interestingly, in relation to age, high body mass index during adolescence or early adulthood has in fact been associated with an increased risk of developing MS later in life. Some studies have also suggested that obesity and comorbid cardiovascular diseases are associated with increased MS susceptibility and worse disease progression[8]. In fact, one study reported that lifestyle-based behavior linked to higher cardiovascular disease was associated with greater central brain atrophy over a 5-year period in MS patients[9]. Another risk factor that influences the disease course of MS is cigarette smoking. This risk factor has been supported extensively in literature, such that one of many studies found smoking less than 5 cigarettes per day for many years implied a two-fold increase risk for developing MS. This same study also found that unlike many other risk factors such as vitamin D deficiency, the Epstein-Barr virus (EBV) infection and obesity to list a few, all of which seem to influence risk during a specific time point in one's life - in particular during adolescence or early adulthood, smoking was not influenced by age, but by

both the duration and intensity of smoking[10]. Other studies with a focus on diet, associated their findings with the gut microbiome, whereby there has been evidence that suggests that the gut microbiota influences the course of MS, such that MS patients exhibit gut dysbiosis. The existing literature on the gut microbiome is often derived from experimental evidence using encephalomyelitis (EAE) mouse models of MS, where it has been reported that people with MS have an altered microbiome, increased intestinal permeability and changes in bile acid metabolism compared to healthy controls. Together, this alters peripheral and CNS immune homeostasis[11]. Epidemiological evidence has also been presented in the literature regarding exposure to the EBV –an established risk factor for MS, that essentially activates human endogenous retroviruses[12]. Interestingly, one recent study reported maternal EBV IgV antibody levels to be associated with risk of MS in the offspring[13]. That said, this study, among many others supports the role of EBV as a risk factor for MS.

Several studies suggest that the risk of developing MS is primarily established in the first decade of one's life, from which the authors inferred that environmental factors act early in life in genetically susceptible individuals, which together triggers the onset of the disease[3]. This is supported by the fact that 10% of MS patients experience their initial demyelinating event during childhood or adolescence[14]. Therefore, the prevailing view is that these environmental risk factors alone do not contribute to MS, but the time in which individuals who are genetically susceptible are exposed, is what prompts the onset of the disease[3].

To quantify genetic risk factors of MS, six twin surveys were conducted in which more than 2000 MS twins were studied. The findings of these surveys suggested that there was a genetic susceptibility with a concordance rate of 25-30% and index of heritability of 0.25-0.76 found in monozygotic twins, ultimately alluding to the idea that there is a much higher

monozygotic than dizygotic twin concordance rate[15]. Apart from twins however, another study found that about 20% of MS patients had at least one relative who had been affected with MS[16]. Although the precise mode of inheritance remains unclear, the disease is understood to neither be Mendelian nor mitochondrial[17]. Furthermore, to date, >200 independent loci across the genome have been associated with MS risk[18]. In fact, of the many genes, the human leukocyte antigen (HLA) classes I and II on chromosome 6, T cell receptor β, cytotoxic T lymphocyte antigen (CTLA)-4, intercellular adhesion molecule (ICAM)-1, and SH2D2A are a few among many to be linked to the onset of MS[16]. Interestingly, many of the risk alleles for MS are shared by several other autoimmune disorders including type 1 diabetes mellitus, rheumatoid arthritis, systemic lupus erythematosus and Crohn's disease, which lends further support to the autoimmune component of MS being an inherited risk[18]. Nonetheless, despite the identification of >200 independent loci across the genome, these seem to only represent a small fraction of the total phenotypic variability in MS, therefore suggesting that it is environmental factors coupled with genetic factors that increases the risks of developing MS[18]. That said, since there is not one specific gene nor one specific environmental factor causing MS; to date, the disease is believed to be multifactorial in nature, involving a combination of both environmental and genetic components.

1.2 Physiology and Pathophysiology of MS

1.2.1 Axonal Injury and Loss

The pathological hallmark of MS are white matter (WM) plaques. These plaques are circumscribed areas of demyelination[17]. Although for many years, MS was considered to be exclusively a WM disorder, mounting evidence now suggests that there is also cortical gray matter (GM) degeneration as well as damage to normal appearing WM (NAWM)[19,20]. Though

the concept of cortical and deep GM lesions in particular, were first introduced in the very early literature of MS pathology by Charcot in 1868, it only gained widespread interest in the last three decades, ultimately leading to the classification of MS as a neurodegenerative disease[21,22]. The idea of MS being a neurodegenerative disease, is based on the extent of axonal loss and neurodegeneration that triggers irreversible disability in the beginning stages of MS. Although demyelination is the hallmark pathology of MS, irreversible axonal loss – thought to be a consequence of demyelination has also been observed. Axonal injury became a topic of popular interest, largely due to the irreversible effects it has[23]. Based on this evidence, one study found that although the relapsing-remitting functional impairments were caused by inflammation and demyelination, the accumulation of an irreversible neurological deficit was caused by axonal destruction and loss[23]. Although demyelination can in part, be repaired through endogenous remyelination, there has been no evidence to date of axon regeneration. That said - even remyelination is not always successful. Though in the earlier phases of MS it could in part be, the extent to which repair can take place is limited by oligodendrocyte survival within plaques, oligodendrocyte precursor cells, not having enough cytokines, growth factors and of course limitations of the underlying demyelination process of MS itself[17]. Conversely, irreversible axonal loss is believed to contribute to the continually worsening neurological deficits that take place in primary and secondary progressive forms of the disease, during which clinical progression corresponds to brain atrophy[24]. In fact, one study found axonal injury to be independent of demyelination[25].

1.3 Clinical Presentation of MS

As discussed earlier in this thesis, disease activity in MS is strongly correlated with the formation of new lesions. These lesions seem to form in various locations throughout the CNS,

rendering the clinical course of MS to follow diverse patterns over time. This precise heterogeneity, as seen in both physical and cognitive outcomes is indicative of the distribution of demyelination within the CNS, and is what results in a diverse range of neurological symptoms attributed to a patient's WM lesions – disseminated in time and space[3,26,27]. A patient typically initially presents with clinically isolated syndrome (CIS) as a first event that may indicate MS. CIS is characterized by either focal or multifocal regions in the CNS, commonly found in the optic nerve, brainstem or spinal cord. This is typically a patient's first episode of inflammation[20]. These CIS patients often present with reversible episodes of neurological deficits that last for days to weeks[1,28]. From there, some CIS patients may or may not ultimately lead to a diagnosis of MS. Typically, those who do begin to develop some neurological deficits, which therefore increase their chances of getting diagnosed with relapsing-remitting MS (RRMS), at which point they will continue to have relapses, with partial or complete recovery. Most of these individuals will ultimately transition to a secondary progressive course in which there is gradual accumulation of disability independent of relapses[1]. Characteristically, patients with MS who present with a more chronic disease progression who go on to develop MS, often begin to present with multifocal lesions within the CNS as seen on MR images, particularly in the periventricular WM, brainstem, cerebellum and spinal cord WM - all of which support a diagnosis for MS[29]. These multifocal lesions then trigger symptoms such as motor weakness, optic neuritis, discoordination, diplopia, numbness, fatigue, depression, reduction in information processing speed and executive functions, and long-term memory deficits to list a few[30]. Taken together, focal WM lesions, WM atrophy and widespread changes in the microstructure of NAWM are the hallmark pathologies of MS[31]. Based on these symptoms, it is clear MS has a substantial impact on one's daily functioning.

1.3.1 Types of MS

The heterogeneous nature of MS, manifested through both physical and cognitive deficits, then created the need to generate a classification system, where the disease could be categorized into three 'types' of MS, namely RRMS, primary-progressive MS (PPMS), and secondary-progressive MS (SPMS) – designed to standardize, facilitate communication, enhance prognostication, and limit heterogeneity in clinical trial populations[32]. The most common form of MS, and the type that most patients typically present with in the earlier course of the disease is RRMS, which affects about 85% of patients[17]. About 10-15% of patients with RRMS experience a relatively mild disease course, and can remain clinically stable for many decades[28]. However, the remainder of those patients typically experience sensory symptoms, Lhermitte's sign (axial or limb paresthesia with neck flexion), limb weakness, gait ataxia, brain stem symptoms fatigue and optic neuritis to list a few – all of which are a result of the demyelination in the CNS[17]. This form of MS is characterized by acute attacks of new or recurrent neurological signs followed by either a complete or partial recovery. RRMS is also separated by periods of stability with no clinical disease activity. Moreover, roughly 10-15% of patients experience PPMS, which is characterized by a gradual progression of neurological disability. The term 'relapse' is considered to be the clinical expression of acute focal or multifocal inflammatory demyelination, disseminated within the CNS[33]. Typically, it is quite common for RRMS patients to gradually evolve into SPMS, in which neurological disability accumulates progressively between or without additional relapses[3,17] Irrespective of the MS type, the two main clinical phenomena of MS are relapses and progression[33]. Likewise, to further build on the idea that every MS patient experiences MS differently, and that not every patient fits into these three types of MS, many studies have sought to understand the mechanisms contributing to MS, to uncover what is causing these individual differences and why some individuals with MS seem to live a relatively

normal life, despite having MS - while others become entirely debilitated. This discrepancy between disease burden and cognitive outcome, where some patients have better preserved cognition than others continues to remain a challenge in the field[22].

1.3.2 The Cognitive Reserve Hypothesis

One study investigated how learning and memory impairments being two prevalent deficits in MS, seem to be weakly associated with MS disease and severity/brain atrophy[34]. From this, the cognitive reserve hypothesis was born. This hypothesis states that both genetic factors (measured through means of maximum lifetime brain growth and quantified by intracranial volume), and environmental factors (measured through various life experiences and quantified through intellect, education, vocabulary and occupational activities) together, contribute to a 'reserve' against disease-related cognitive decline. Together, from this, several studies inferred that higher lifetime intellectual enrichment lessens the negative impact of MS disease severity (i.e. brain atrophy) on learning and memory and ultimately explains why there is a disconnect between brain disease and cognitive status in neurologic populations like that of MS - which could explain why some people are not as affected by their MS as others. Several other studies did in fact support this hypothesis[35,36,37]. Together, this could pave the way for potential preventative measures used for those more susceptible to developing MS[34,36,37,38]. Thus, with no known cause or cure, this debilitating disease renders it difficult for individuals to function in all aspects of their lives, making MS a life altering disease - and fairly unpredictable in nature.

1.4 MS Diagnosis: Imaging and Clinical Assessments

1.4.1 Imaging: Magnetic Resonance Imaging (MRI)

Over the past few decades, with the advent and widespread availability of Magnetic Resonance Imaging (MRI) systems, brain imaging has gained an increasing role in both MS

diagnosis and research[39]. This is largely in part due to MRI being a powerful noninvasive imaging modality that uses strong magnetic fields to produce images of biological tissue. Fundamentally, diagnosing MS is largely based on the demonstration of the dissemination of demyelinating lesions to various regions across the CNS (dissemination in space (DIS)) and over time (dissemination in time (DIT)).

WM disorders such as that of MS have historically used MRI as a primary diagnostic tool. However, MRI methods have come a long way since the 1980s. Historically, imaging biomarkers have struggled to predict specific symptoms and their severity. In fact, a concept known as the 'clinicoradiological paradox' refers to the weak correlation of MRI lesion load with clinical disability, describing its reduced value as a prognostic marker for clinical impairments[30,40,41]. This notion has now unsurprisingly proved to be a paradox, owing to MRIs sensitivity to MS-related abnormalities, non-invasiveness, reproducibility and repeatability[42,43]. This association between clinical findings and the radiological extent of involvement has now led to MRIs prominent role in diagnosing MS, and is now a powerful diagnostic tool for detecting and measuring lesions, assessing brain atrophy and evaluating WM and GM MS pathology[20,41].

Despite the widespread use of the MRI as a powerful diagnostic tool, its use remains limited when trying to decipher some of the neural mechanisms underlying cognition in diseases like MS. Studies that have used conventional MRI have found it challenging to investigate something as complex as cognitive impairment in MS on just the basis of T2 lesional disease burden. Therefore, although conventional MRI has effectively proven to quantify structural brain damage, WM and GM pathology outside of damaged tissue, in areas known as NAWM and NAGM it becomes challenging to quantify, and therefore requires more advanced quantitative

neuroimaging techniques. Because of this, the use of more advanced quantitative MRI techniques is now becoming increasingly common, as they allow for the visualization of widespread abnormalities in the CNS - beyond WM focal lesions, which ultimately broadens our understanding of the neurodegenerative disease process[44]. These quantitative measures which are highly sensitive in detecting MS plaques, provide quantitative assessments of inflammatory activity and lesion load, which is essential in times when MS-related abnormalities go undetected with conventional MRI - which is often the reason why modest correlations are reported between MRI-visible WM lesions and neurological deficits[33,44]. Some of these advanced quantitative MRI methods include diffusion tensor imaging (DTI)[45], magnetization transfer imaging (MTI)[46] and myelin water imaging (MWI)[47] to list a few, which have allowed us to look at the microstructural, metabolic and functional changes in MS patients – moving closer toward understanding the variables giving rise to the complex manifestation of diseases like MS[44]. DTI imaging in particular, which will be discussed in more detail later in this thesis, has advanced the field of brain imaging with the ability to obtain reliable in vivo estimates of brain damage, suggesting that MS is not limited to lesions visible on T2-weighted images as seen by conventional MRI, but instead has demonstrated that several brain regions that may appear 'normal' (i.e. NAWM) on conventional MRI, are in fact driving some of these cognitive deficits. In fact, in addition to NAWM merely driving some of these cognitive deficits, several DTI studies have reported damage in specific WM tracts to be associated with EF decline, as supported by poor performance on the Paced Auditory Serial Addition Test (PASAT), The Multiple Errands Test (MET) and the Trail Making Test (TMT) and Color Word Interference Test (CWIT) from the DKEFS Test[20]. Together, this suggests a clear association between DTI and NAWM in MS, and therefore suggests that conventional MRI is not sufficient in

understanding more complex cognitive deficits in persons with MS. Similarly, among many, one such study reported increased MD in NAWM over a 15-month period in persons with MS - independent of lesion load and brain volume. These findings were then further supported by other findings that reported that changes in NAGM occur over time, independent of whole brain and GM volumes[48,49]. Taken together, it is evident through the extent of damage in NAWM and NAGM, that there seems to be damage beyond what conventional MRI methods can detect. This then created the need to investigate brain damage beyond what is seen by conventional MRI, therefore paving the way for MS studies to then employ more advanced quantitative MRI methods as mentioned above, in hopes to work toward better understanding anatomical connectivity patterns to enhance our understanding of the relationships between MRI findings and specific cognitive deficits and the corresponding brain networks that are affected[50]. However, despite how far we have come by employing more advanced quantitative imaging methods in studying MS, these studies are often predicated on precise one-to-one spatial mappings between the brain images of different individuals. This is often done through warping each participant's brain to that of a commonly used brain template which enables researchers to conduct region of interest analyses and group-wise comparisons. However, with MS studies in particular, the presence of MS lesions and other MS-related brain pathologies seem to affect the accuracy of automated warping methods - also known as spatial normalization. Chapter 3 of this thesis, will therefore work to address this gap.

1.4.2 Diffusion Tensor Imaging

One powerful quantitative MRI method that revolutionized the visualization of WM structures by exploiting the properties of water diffusion is DTI imaging. This method originally introduced in 1994 by Basser et al., measures the displacement of water molecules on a micro

scale, ultimately providing information about the WM fibers that pass within a pixel[45,51]. Since water molecules in the human body undergo a random Brownian motion - typically influenced by partially permeable barriers and structures, DTI then works to quantify the relative diffusivity of water in a voxel into directional components, which is in turn affected by the magnitude and directionality of diffusion[51,52]. The restriction of water molecule movement depends on the direction in which the diffusion is measured. This property is known as anisotropy and results in greater diffusion along axons in comparison to the transversal measurement. DTI also provides brain maps of the magnitude of diffusion - reflected by the mean diffusivity (MD), and the degree of anisotropy as mentioned above - termed fractional anisotropy (FA)[53]. These two scalar maps are used to quantify diffusion properties. MD values reflect the average rate of molecular diffusion, such that higher values of MD correspond to higher diffusivity and vice versa. Conversely, FA can be computed for each voxel expressing the preference of water diffusion in an isotropic or anisotropic manner. The term isotopic can be understood as there being no restrictions on diffusion, such that molecules will diffuse equally in all directions, and anisotropic is a process whereby there are no restrictions on diffusion, where diffusion may occur along one axis. For instance, in WM, anisotropy is high, meaning the water molecules diffuse fastest along the length of the fiber and the slowest perpendicular to them/across the width of the fiber. Moreover, FA values are relative measures that can range between values of 0-1. Values closer to 1, indicate that nearly all the water molecules in the voxel are diffusing along the same preferred axis (anisotropic diffusion), whereas values closer to 0, indicate that the water molecules are equally likely to diffuse in any direction (isotropic diffusion). One of the advantages of using DTI is that it is rotationally invariant, meaning it can measure the principle

diffusivities regardless of the position of the fibers in space. Therefore, it can extract both the magnitude of the diffusivities and also their 3D alignment[45].

1.4.2.1 Application of DTI Measurements with MS

In relation to MS, previous DTI studies have shown that as WM tracts undergo demyelination or axonal loss, their microstructure is disrupted, which in turn alters the diffusion of water. Previous studies have also shown that higher MD values with lower FA values in acute plaques are likely indicative of edema, demyelination, axonal loss and an overall increase in barrier permiability[40]. Thus, since MS is a demyelinating disease, DTI plays a pivotal role, as the myelin within the WM is believed to be one of the main drivers of the DTI signal. That said, although it is clear that there is a significant amount of potential for DTI studies to enhance our understanding of MS, the complex manifestation of the disease renders it difficult to do so to its full potential. Despite the commonality of most MS patients experiencing chronic progression, the complexity of MS results in a diverse range of neurological symptoms experienced by patients – leading to unique MS experiences all around[27]. This in turn creates a need for uncovering the variables giving rise to these individual differences in cognition, and particular executive function. Therefore, to advance our understanding of this variability, Chapter 4 will highlight some of the underlying factors contributing to these individual differences seen in cognitive performance using DTI measures.

1.5 Clinical Assessments

With the ability of advanced quantitative MRI methods to detect disease-related abnormalities and specifically its proven sensitivity to detect demyelinating lesions, we are able to use reliable imaging modalities in conjunction with a variety of clinical assessments, which together enhance diagnosis and leads to many new avenues that work to reduce disease activity,

and in part progression[1]. Likewise, a criterion from the 1980s known as the Poser Criteria was typically used as diagnostic criteria. To fit this criteria, a patient needed to present evidence of at least two relapses - in line with typical MS symptoms and have evidence of some sort of involvement of WM in more than one region of the CNS[54]. Since then however, this model has been replaced by the McDonald criteria, which itself has been revised in May of 2017. This system requires patients to have lesions that affect at least two distinct sites in the CNS with two episodes of neurological symptoms separated in time, for which there is no better reason for their clinical presentation[55]. Unlike the Poser criteria, the revised McDonald Criteria allows for a more rapid diagnosis and improved specificity and sensitivity. Ultimately this revised criteria allows for a simpler diagnostic process with fewer MRI examinations[39].

As the field of MS advances, efforts have been made to gage a more holistic picture of MS. To do so, various rating scales have been used in conjunction with MRI methods. Some of which include the Expanded Disability Status Scale (EDSS) and the Multiple Sclerosis Functional Composite (MSFC). In fact, of the two, Kalkers et al., investigated the relationship between the new MSFC and MRI lesion load as a biological disease marker and found that the MSFC correlated better with both T2 hypointense and T1 hypointense lesion load than the EDSS[56]. Other studies have worked to further prove the strong association between cognitive function and MRI measures, such as Edwards et al., who found a clear relationship between cerebral atrophy and cognitive performance by suggesting an association between MRI volume estimations and cognitive deficits by correlating WM volumes with global Cognitive Index Scores (CIS)[57].

1.5.1 Cognition

Cognitive impairment affects 40-70% of individuals with MS - rendering it to be a major cause of disability. To understand cognition in MS, it is integral to first understand some of the domain-specific cognitive processes that influence neurocognitive domains such as attention, EF and memory to list a few. This is largely because cognitive deficits in MS are domain-specific, as opposed to contributing to global cognitive decline. Interestingly, these domain-specific deficits in MS, result in considerable variability in the frequency and pattern of impairment among MS patients[58].

According to the DSM-5 approach, some of the primary neurocognitive domains include complex attention, EF, language, perceptual-motor function, learning and memory and social cognition. Clinically, attentional behavior refers to the ability to choose a task on which to attend (selective attention), in order to utilize mental resources focused on a specific task, despite being surrounded by distractions (focused attention), to ultimately sustain attention on a specific task over long periods of time (sustained attention). Attention deficits in MS have been observed in up to 25% of patients[59]. Moreover, speed of information processing refers to the ability to maintain and manipulate information for a short period of time, and to the speed in which one can then process that information. This key deficit is seen in about 20-30% of MS patients[60]. Interestingly, several studies on MS have grouped together deficits in attention and speed of information processing, and have found associations between attention and speed of information processing and GM atrophy of strategic brain structures directly (such as the thalamus and cerebellum) or indirectly through control of visual functions such as in the putamen and occipital cortex involved in cognitive function[61]. EF impairment in contrast, is seen in up to 25% of patients and can be observed through tasks involving planning, problem solving, executing task strategies, decision-making, inhibition and flexibility to list a few[62]. Broadly, EF refers to

maintaining higher-level control over behavior and higher level reasoning[60]. Several studies have suggested that MS patients consistently demonstrate impaired EF in comparison to controls due to their impaired problem solving strategies and concept formation[59]. In fact, two studies reported that MS patients performed poorly on two tasks of EF - both the Wisconsin Card Sorting Test (WCST) and the Sorting Test from the DKEFS, which were shown to be correlated with increased lesion load and atrophy, as assessed by MRI[63,64]. Moreover, perceptual-motor function can be assessed through visual perception, visuoconstructional reasoning and perceptual-motor coordination. Deficits have also been reported in verbal abilities, which can be observed through speech comprehension. One instance in which deficits in impaired comprehension of language can be observed, is through a patient's difficulty in responding to a set of questions or given instructions. This however can also be a result of deficits in other domains such as attention and executive functioning[65]. Language can be assessed through object naming, word finding, fluency, grammar and syntax and receptive language. Learning and memory however can be observed through free recall, cued recall, recognition memory, long-term memory and implicit learning. The California Verbal Learning Test II (CVLT) II is a neuropsychological test often administered on MS participants to assess episodic verbal learning and memory. This test asks MS participants to remember a word list, whereby the administrator can then observe how they choose to recall those words through strategy or conceptual inference[65,66]. Memory and learning disturbances in MS appear to be quite frequent, with impaired memory seen in 40-65% of patients[67]. Memory impairments can be separated into different domains including episodic memory (personally experienced events), working memory (inability to retain information due to difficulties in concentration or attention) and semantic memory (word meaning and general knowledge)[68]. Most patients however typically present with

impairments in their short-term and working memory[67]. Several studies have also reported fatigue as a symptom commonly experienced among patients, in which it could be inferred that perhaps fatigue is one of many factors contributing to poor cognitive performance[59]. Taken together, cognitive dysfunction in MS is a result of a series of domain-specific disconnections. The disruption of the WM tracts appears to lead to reduced functional connectivity between cortico-cortical and cortico-subcortical cognitive processing regions, that together result in impairments in specific cognitive domains[69].

1.5.2 Executive Function

Roughly 17-25% of MS patients have difficulties in higher order executive functions[62]. Anatomically, EF relies primarily on the integrity of the prefrontal cortex and its connections with other cortical and subcortical systems. Diagnosing impairments in this domain however can be understood as engaging in purposive, self-serving behavior, and often leads to a patient's inability to set goals, think conceptually, verbal fluency, make plans and organize. Therefore, a patient's impaired control over their thoughts, behaviors and emotions affects not their ability to maintain daily functioning, but to also sustain independent living.

Historically neuropsychological tests assessed several interrelated domains and regions of the brain. One domain-specific test known as the Delis-Kaplan Executive Function System (DKEFS) test has systematically been suggested to be the most robust test for measuring EF decline, such that it assesses a much wider range of independent executive abilities, over previous EF tests in MS. Among many studies, one large-scale New Zealand study conducted a comprehensive assessment of EF, general cognitive ability and memory by performing all subtests of the DKEFS using 95 MS participants. This study not only suggested that MS participants perform more poorly on tests of EF, but their findings also suggested that the

DKEFS allowed for a much more comprehensive assessment of EF than previous methods. Taken together, this study's findings supported the robustness of DKEFS when assessing EF dysfunction[70]. These findings were lent further support by another study that found scores from the DKEFS sorting test to be significantly lower than healthy controls, whereby MS patient scores were a result of fewer sorts, a smaller description score and more redundant sorts[63]. In addition to these studies done on adult onset of MS, one study that used DKEFS in a pediatric MS cohort, also found DKEFS to be more robust in assessing EF, than previous tests such as the Stroop Test or the Tower of London Test[71]. Taken together, DKEFS, unlike many other neuropsychological tests, assesses EF exclusively, as opposed to other tests that assess a compound of various cognitive functions such as processing speed and working memory, rendering it difficult to isolate the effects of EF on a given test[59]. Interestingly, in addition to MS, other patient populations like Parkinson's disease, Schizophrenia and Schizoaffective disorder all seem to use DKEFS when assessing EF[72,73]. That said, despite the identification of a robust method of measuring EF decline, there still remains gaps in understanding the complexity of EF dysfunction in MS, largely due to inconsistent findings and incomparable studies in the literature. Because of this, Chapter 4 of this thesis will work to further address EF dysfunction in MS.

Understanding the mechanisms underlying cognitive impairment in MS have been moderately explored in the literature, through means of better understanding the structural and functional connectivity patterns that underlie these domain-specific impairments. In fact, a meta-analysis performed on data from 495 patients across 12 different studies, seven of which focused on DTI imaging studies, found impaired cognition to be significantly associated with lower FA in the callosal genu, thalamus, right posterior cingulum and fornix crus. The findings from this

meta-analysis provide insight into how widespread WM damage is. In line with the literature, this study's findings of lower FA relating to cognition, support the importance of understanding the functional and structural connections in the MS brain[74,75]. Taken together, both advanced quantitative MRI methods coupled with robust neurocognitive assessments are now used in conjunction with one another to enhance our understanding of cognitive impairment in MS. Chapter 4 of this thesis will therefore work to investigate the correlations between brain structure, EF and cognition, to uncover the associations between MRI findings and EF decline.

Chapter 2: Hypotheses and Objectives

2.1 Problem Statement

The purpose of this thesis is to contribute to the understanding of how brain microstructure, as defined by DTI-based fractional anisotropy (FA) and mean diffusivity (MD) relates to individual differences in cognitive impairment in MS. This will be done by employing a network based approach, as high-level control processes have been suggested to rely on the integrity of, and dynamic interactions between core neurocognitive networks[76]. The functional interactions between these brain networks has provided insight into the associations between structural and functional connectivity changes to that of clinical deficits and overall cognitive performance. This however has been made possible through the use of anatomically-defined WM atlases and WM probability maps of the brain[77]. This thesis will therefore employ a network based approach to highlight how WM microstructure within two functionally-defined brain networks, namely the DMN – a highly activated brain network during resting state and deactivated during execution of working memory and attention cognitive tasks[78] and the ECN – a network involved in executive functions such as control processes and working memory[79] as well as lesioned and NAWM, correlate with individual differences in EF decline. This will ultimately improve our understanding of the underlying causes of MS-related cognitive decline, by establishing neural correlates underlying individual differences in cognitive performance in MS.

2.2 Rationale

Despite the fact that 40-70% of MS patients suffer from cognitive impairments, individual risk factors for cognitive disability remain largely unknown, and there are currently no reliable prognostic markers to identify patients who are likely to develop cognitive deficits, rendering it difficult to manage disease-related cognitive decline before it progressively worsens.

One barrier however, in overcoming this gap in the field is that several of the spatial normalization algorithms and brain templates that have been developed so far, have only been done on studies using neurologically healthy individuals. No previous studies have systematically compared normalization methods to evaluate their performance in the presence of MS-related pathologies. Therefore, in the absence of established 'best'-practice' guidelines for spatially normalizing brain imaging data in the presence of MS pathologies, it became imminent to determine a processing pipeline that would enable the most reliable comparisons between individuals or groups in MS neuroimaging studies. Therefore, once a robust method is identified that can yield more accurate voxel-wise and ROI-based comparisons between MS individuals or groups, all MS studies can then adopt a uniform image processing pipeline to allow for more accurate comparisons between studies and facilitate future meta-analyses. Establishing a data processing pipeline that can enable the most reliable comparisons between individuals or groups in MS neuroimaging studies, will then lay the foundation to explore different WM pathways and possible regions that correlate to various cognitive deficiencies, allowing us to draw inferences on cognitive performance and WM microstructure using our new functionally defined WM Atlases. Taken together, this approach will highlight how individual differences relate to cognitive performance, and ultimately establish how microstructure correlates to cognition in MS. By uncovering correlations between microstructure and cognition, we can shed light on the underlying causes of MS-related cognitive decline, and specifically that of EF decline.

2.3 Aims

This study will aim to first identify the most robust method to yield accurate voxel-wise and ROI-based comparisons between MS individuals or groups by establishing a uniform image processing pipeline. This pipeline will then be used to define 111 participant's executive function

as the contrast between the most executive sub-component of the DKEFS Color-Word Interference Test (i.e. inhibition/switching tasks) vs. the two baseline measures (i.e. Condition 1: combined color naming and Condition 2: word reading tasks). This work will ultimately expand our understanding of how individual differences in brain microstructure, as defined by DTI-based fractional anisotropy relate to cognitive performance.

2.4 Hypotheses

The following thesis will test the following two hypotheses: 1) that nonlinear warping methods in conjunction with lesion-filling will outperform conventional linear (affine) normalization 2) that there will be a positive correlation between individual differences in executive function and WM microstructure within the DMN and ECN, where participants with higher executive function will have lower MD values and higher FA values.

Chapter 3: Comparing spatial normalization algorithms for brain MRI data with multiple sclerosis pathologies

Running Title: Spatial normalization in the presence of MS brain pathologies

Abstract Word Count: 292

Manuscript Word Count: 4,202 (excluding the Abstract, Table/Figure Captions and References)

Number of Primary Tables and Figures: 0 Tables; 5 Figures

Number of Supplementary Materials: 1 Supplementary Figure and 1 Supplementary Table

Keywords: Brain; Lesion; Multiple Sclerosis; MRI; Spatial Normalization; Warping; MRIStudio; FSL; ANTs; SPM.

3.1 Abstract

Background: Spatially normalizing brain MRI data to a template is commonly performed to facilitate comparisons between individuals or groups. However, the presence of multiple sclerosis (MS) lesions and other MS-related brain pathologies may compromise the performance of automated spatial normalization procedures. We therefore aimed to systematically compare five commonly used spatial normalization methods for brain MRI – including linear (affine), and nonlinear MRIStudio (LDDMM), FSL (FNIRT), ANTs (SyN), and SPM (CAT12) algorithms – to evaluate their performance in the presence of MS-related pathologies.

Methods: 3 Tesla MRI images (T1-weighted and T2-FLAIR) were obtained for 20 participants with MS from an ongoing cohort study (used to assess a real dataset) and 1 healthy control participant (used to create a simulated lesion dataset). Both raw and lesion-filled versions of each participant's T1-weighted brain images were warped to the Montreal Neurological Institute template using all five normalization approaches for the real dataset, and the same procedure was then repeated using the simulated lesion dataset (i.e., total of 400 spatial normalizations). As an additional quality-assurance check, the resulting deformations were also applied to the corresponding lesion masks to evaluate how each processing pipeline handled focal white matter lesions. For each normalization approach, inter-subject variability (across normalized T1-weighted images) was quantified using both mutual information (MI) and coefficient of variation (COV), and the corresponding normalized lesion volumes were evaluated using paired-sample t-tests.

Results: All four nonlinear warping methods outperformed conventional linear normalization, with SPM (CAT12) yielding the highest MI values, lowest COV values, and proportionately-scaled lesion volumes. Although lesion-filling improved spatial normalization accuracy for each

of the methods tested, these effects were small compared to differences between normalization algorithms.

Conclusions: SPM (CAT12) warping combined with lesion-filling is recommended for use in future MS brain imaging studies requiring spatial normalization.

3.2 Introduction

Multiple Sclerosis (MS) is a neurodegenerative disorder of the central nervous system characterized by focal lesions and atrophy in both white matter (WM) and grey matter (GM) regions[80]. Several quantitative MRI methods such as diffusion tensor imaging (DTI)[81], magnetization transfer imaging (MTI)[46], and myelin water imaging (MWI)[47] have been widely adopted to study MS and other WM disorders[82,83]. Such studies are often predicated on precise one-to-one spatial mappings between the brain images of different individuals. This is typically achieved by warping each participant's brain image to a common template, which then facilitates voxel-wise or region of interest (ROI)-based comparisons between individuals or groups[84]. However, among participants with MS, widespread brain pathologies (e.g., focal WM and GM lesions, distributed WM and GM atrophy, altered normal appearing white matter signals, etc.) are likely to affect the accuracy of automated spatial normalization methods.

Several spatial normalization algorithms and brain templates have been developed for studies of neurologically healthy individuals[85], but no previous studies have systematically compared normalization methods to evaluate their performance in the presence of MS-related pathologies. Generally, these approaches aim to minimize differences between each participant's data and a template image, such as Talairach and Tournoux or Montreal Neurological Institute (MNI) templates[86], using linear and/or nonlinear spatial transformations[87,88]. Linear transformations apply the same translation, rotation, and scaling parameters to all voxels within an image. Although they are robust to local pathologies, they do not accurately match individual brain structures, particularly in WM and other sub-cortical regions that are of particular interest in MS[89]. Conversely, nonlinear transformations apply different scaling parameters to each voxel. This allows more localized region-specific deformations, but the high-dimensional nature of these algorithms renders them prone to over-fitting during the template matching process, which

can reduce or eliminate abnormal but potentially salient features in the images (e.g., erroneously increasing or decreasing sizes of focal brain lesions)[84,89,90].

To minimize these types of erroneous spatial deformations, brain lesions in clinical populations are often identified and either discounted (aka, 'de-weighted') during spatial normalization or lesion-filled (aka, 'in-painted') by intensity-correcting them based on signals from neighboring, normal-appearing tissue before spatial normalization[91]. Lesion-filling has been shown to improve anatomical correspondence, as well as WM and GM volume measurements among participants with MS[92,93].

Although studies comparing different image processing pipelines and spatial normalization methods have revealed performance differences in Alzheimer's disease, mild cognitive impairment, drug-resistant epilepsy, and stroke[84,94], no such comparisons have been reported for MS. Therefore, in the absence of established 'best-practice' guidelines for spatially normalizing brain imaging data in the presence of MS pathologies[84,89], we aimed to: 1) use MS brain imaging data to systematically evaluate the performance of five commonly-used spatial normalization approaches in four popular neuroimaging software packages including MRIStudio, FSL, ANTs and SPM, before and after lesion-filling; 2) create a simulated lesion dataset to compare how each normalization approach was specifically affected by focal lesions rather than global differences in brain volumes and GM/WM signal intensities; and 3) determine a data processing pipeline that would enable the most reliable comparisons between individuals or groups in MS neuroimaging studies.

3.3 Materials and Methods

3.3.1 Data Acquisition

The current study used de-identified MRI images from 20 randomly selected participants with MS [16 female; range 22-66 years] and one randomly selected neurologically healthy control participant enrolled in the ongoing Comorbidity, Cognition and Multiple Sclerosis (CCOMS) Study[95]. The study was approved by our institutional Research Ethics Board and written informed consent was obtained from all participants. All participants with MS (19 relapsing remitting; 1 secondary progressive) were diagnosed by neurologists delivering specialized MS care using the revised McDonald criteria[96]. MS participants all had Expanded Disability Status Scale (EDSS) scores between 1.0-6.5 [mean±SD = 2.88±1.45], and disease durations between 1-23 years [mean±SD = 12.05±7.41 years][97].

All brain imaging data were acquired using a Siemens Tim Trio 3T MRI system with a 32-channel head coil (Siemens Healthcare, Erlangen, Germany). Each MRI examination included a whole-brain T1-weighted (T1w) MPRAGE (Repetition Time [TR] = 1900 ms; Echo Time [TE] = 3.46 ms; Inversion Time [TI] = 900 ms; Flip Angle = 9°; Matrix Size = 256 × 256; Number of Slices = 176, Field Of View [FOV] = 250 × 250 mm2; Voxel Size = 0.98 × 0.98 × 0.98 mm3; Acquisition Time [TA] = 4:26 min) and a whole-brain T2-weighted fluid-attenuated inversion recovery (T2-FLAIR) sequence (TR = 9000 ms; TE = 100 ms; TI = 2499.2 ms; Flip Angle = 130°; Matrix Size = 256 × 256; Number of Slices = 32; FOV = 240 × 240 mm2; Voxel Size = 0.94 × 0.94 × 4.00 mm3; TA = 5.06 min).

3.3.2 Image Processing

We chose to compare four software packages that are well established, freely available, and widely used throughout the neuroimaging research community in order to ensure that our

findings could be replicated and would be of value in future MS neuroimaging studies. The following software packages were included: MRIStudio version 1.9 (https://www.mristudio.org/, Johns Hopkins University), FSL version 5.0.10 (https://fsl.fmrib.ox.ac.uk/fsl/fslwiki/, University of Oxford), ANTs version 2.1.0 (http://picsl.upenn.edu/software/ants/, University of Pennsylvania), and SPM12 version 7219 (http://www.fil.ion.ucl.ac.uk/spm/software/spm12/, Wellcome Trust Centre for Neuroimaging) with the Computational Anatomy Toolbox for SPM12 (CAT12 version R1148; http://www.neuro.uni-jena.de/cat/, University of Jena). All image analyses were performed on a Macintosh computer (OSX 10.13.6 High Sierra operating system).

3.3.2.1 Skull Stripping

Each participant's raw T1w MRI image in subject space was 'skull-stripped' using FSL's automated brain extraction tool (BET) with a fractional intensity threshold of 0.45 to separate brain from non-brain tissue[98]. This brain extraction step has previously been shown to improve subsequent normalization of structural MRI data in both healthy and clinical populations[99].

3.3.2.2 Lesion Filling

Automated lesion segmentation was performed using the Lesion Segmentation Toolbox (LST) for SPM12 (http://www.statistical-modelling.de/lst.html, Technical University München). The T1w and FLAIR images were linearly co-registered before applying the lesion growth algorithm (LGA) using the T1w and FLAIR signal intensities and a kappa threshold of 0.2[100]. The binary lesion masks and normal appearing white matter (NAWM) masks from the LST were then used to create lesion-filled T1w images via the FSL 'lesion_filling' command[93].1

[1] The combination of SPM and FSL was intentionally employed here to avoid all of the image processing being performed within any single software package (which could potentially bias the subsequent normalization results in favor of that package).

3.3.2.3 Spatial Normalization

Each of the 40 skull-stripped T1w images (i.e., 20 before lesion-filling and 20 after lesion-filling) were spatially normalized to 1.0 × 1.0 × 1.0 mm3 T1w MNI templates using each of the following five spatial normalization approaches (**Figure 3.1**). Each software package's included T1w MNI template and default parameters were used, unless otherwise noted.

1. *Linear (Affine)*: Linear spatial normalization was achieved by applying a 12-parameter affine (AIRLinear) transformation using the DiffeoMap Toolbox in MRIStudio[101].

2. *MRIStudio (LDDMM)*: After an initial linear (affine) normalization within the DiffeoMap Toolbox (described above), nonlinear warping using the large deformation diffeomorphic metric mapping (LDDMM) algorithm[102] was implemented with cascading alpha values (i.e., 0.01, 0.005, 0.002) to allow increasingly elastic deformations, as previously described[77].

3. *FSL (FNIRT)*: After an initial linear (affine) normalization using FSL's Linear Image Registration Tool (FLIRT)[103,104], nonlinear spatial normalization was performed using FSL's Nonlinear Image Registration Tool (FNIRT)[105].

4. *ANTS (SyN)*: Nonlinear spatial normalization was performed using the Advanced Normalization Tools (ANTs) Symmetric Normalization (SyN) algorithm[106], which combines linear and nonlinear bidirectional mappings.

5. *SPM (CAT12)*: Nonlinear spatial normalization was performed using the CAT12 Toolbox [107] within SPM12, initially using low-dimensional nonlinear warping, followed by a two-stage nonlinear normalization approach based on Geodesic Shooting algorithms[88,108].

Figure 3.1: Image processing pipeline

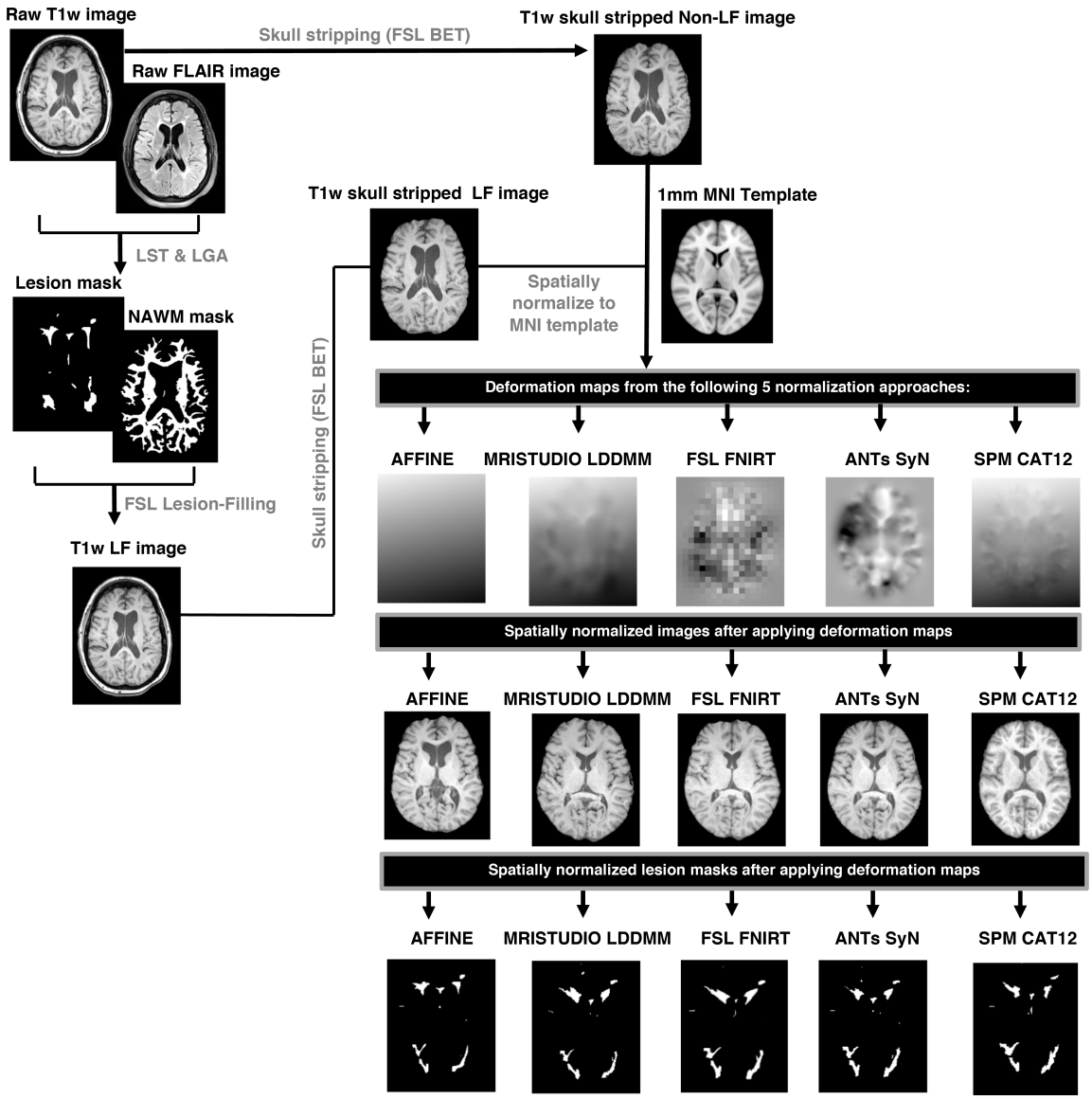

Figure 3.1: Comprehensive image-processing pipeline for warping the T1w MRI images and lesion masks from each participant to the Montreal Neurological Institute (MNI) brain template. Spatial normalizations were performed using five commonly used algorithms, both before and after lesion-filling the T1w images. Note: Axial brain images are displayed in neurological convention (left=left); NAWM: normal appearing white matter, LST: lesion segmentation toolbox, LGA: lesion growth algorithm, Non-LF: non lesion-filled, LF: lesion-filled.

Although some of these software packages are able to generate normalized T1w images directly, such images may have been subjected to additional, interim processing steps such as smoothing, interpolation or global intensity scaling. Therefore, rather than using direct outputs from any of the software packages, the resulting deformation fields from each algorithm (after combining the linear and nonlinear deformations, if applicable) were applied to each participant's original T1w image. This was done either before or after lesion-filling, but without any additional processing steps, and was also done to the corresponding LST-segmented lesion masks. The aim was to yield the most direct comparison between the algorithms themselves, and to limit other potential differences between the image processing pipelines and software packages.

3.4 Methodological Comparisons

We used three measures to assess spatial normalization accuracy, before and after lesion-filling with each normalization algorithm, including: 1) mutual information (MI) between normalized images; 2) coefficient of variation (COV) between normalized images; and 3) volume of spatially-normalized lesion masks. Comparing the similarity of warped images using MI and COV values reflects how well each normalization procedure worked in terms of making all participants' images look the same; however, tracking the lesion volume is also important to ensure that successful spatial normalization was not achieved by, or at the expense of, inappropriately shrinking or expanding focal lesions.

To measure the similarity between spatially normalized T1w images that were generated using each approach, we first calculated MI, I(X;Y), for all combinations of image pairs within each group ($\frac{20!}{2!\,(20-2)!} = 190$) using the freely-available Fast Mutual Information of Two Images or Signals Toolbox in Matlab (https://www.mathworks.com/matlabcentral/fileexchange/13289-

fast-mutual-information-of-two-images-or-signals). Each of the raw MI values were then scaled between [0,1] by dividing them by the absolute upper bound, UX, defined by I(X;X) – based on the principle that any given image, by definition, contains as much or more mutual information about itself compared to any other image ($\frac{I(X;Y)}{U_X} = \frac{I(X;Y)}{I(X;X)}$) [109]. Thus, higher scaled MI values indicate greater similarity between images, with 0 indicating that images are completely independent (i.e., no correspondence between X and Y) and 1 indicating that images are completely dependent (i.e., 1:1 correspondence between X and Y) although not necessarily identical (e.g., allowing for global differences in contrast and/or signal intensity between X and Y).

Then, to quantify and visualize the degree of overlap between the spatially normalized images, COV maps were generated for each normalization approach by dividing the standard deviation by the mean T1w signal intensity in a voxel-wise manner across all 20 images in each group (i.e., dataset/algorithm/lesion-filling condition). Overall performance was then quantified by calculating the average COV across all voxels within the brain, such that well-aligned sets of images (in which tissue types and signal intensities in each region are closely matched across participants) have lower overall COV values.

However, while higher MI and lower COV are generally desirable, these measures alone do not reflect whether each normalization algorithm adequately deals with focal lesions. For example, images from different participants could theoretically be made to look more similar by reducing the variability caused by focal lesions (e.g., by shrinking them within NAWM or expanding them into ventricular regions). Thus, in order to evaluate the degree to which overall lesion volumes were preserved (i.e., scaled proportionally) during each spatial normalization, we

calculated the 3D volume of each warped lesion mask, and performed comparisons between methods using two-tailed paired t-tests.

All statistical analyses were performed using MATLAB (version 2015a, The MathWorks Inc., Natick, MA, USA) and MedCalc 17.2 (MedCalc Software, Mariakerke, Belgium).

3.4.1 Validation and Lesion-Specific Analyses Using Simulated Brain Lesion Data

In addition to analyzing brain images of the 20 participants with MS, a simulated brain lesion dataset was generated for cross-validation and to examine the performance of each spatial normalization algorithm in the presence of focal WM lesions alone. Instead of using each participant's raw brain images, which include inter-subject differences in GM, WM, and cerebrospinal fluid (CSF) volumes, NAWM intensities, as well as focal lesion locations and volumes, the simulated dataset was generated by transposing WM lesions from each participant with MS onto a reference T1w image from one randomly selected neurologically healthy study participant. An in-house MATLAB code, along with the healthy participant's WM mask, was used to ensure that the imposed lesions were within the brain parenchyma and primarily restricted to WM regions – thereby producing a set of 20 images differing only in lesion location, volume, and intensity, while controlling for volume and signal intensity throughout GM, CSF and NAWM regions. Each of these images then underwent the same five spatial normalization approaches, before and after lesion-filling as described previously for the MS participant data, and the resulting deformation fields were then applied to the original reference T1w image without any lesions. Applying each of the resulting deformations to the same control image in this simulated dataset thereby provides a 'ground truth', where all of the warped images should have the same geometric properties and image intensities (i.e., MI should be 1 and COV should be 0) except for differences that result from spatial normalization of the images in the presence

of focal lesions. Although similar approaches have been taken in previous studies, one recent MS study in particular, also used a simulated dataset to run their experiments and ultimately validate their findings[110]. Therefore, results obtained from the use of a simulated database do seem to provide valuable insight, by providing a 'ground truth'.

3.4.2 Visualizing Differences at the Single-Subject Level

Finally, we chose one MS participant (same as shown in Figure 1) to briefly illustrate some of the differences between normalization methods at the single-subject level. To do so, we applied the inverse deformations from each method, based on non-lesion-filled images, to the popular and freely-available JHU-MNI-ss atlas (aka, 'Eve Atlas')[111] using nearest-neighbor interpolation. After warping the atlas into subject-space, the anatomical volumes of two deep GM structures (caudate and thalamus) and two deep WM structures (genu and splenium of the corpus callosum) were quantified based on the respective brain parcellations that resulted from each normalization method. Finally, we used the Dice similarity coefficient (DSC)[112], ranging from 0 (no overlap) to 1 (exact overlap), to quantify the degree of spatial overlap between a binarized mask of all four structures from each normalization approach.

3.5 Results

In total, 400 spatial normalizations were performed on the MRI datasets (20 images x 5 spatial normalization algorithms x 2 lesion-filling conditions x 2 patient/simulated datasets). Since some spatial normalization algorithms were more computationally intensive than others, ranging from ~1 minute/participant for linear (affine) to ~60 minutes/participant for MRIStudio (LDDMM), approximate processing times for each approach and exact version numbers for each software package are shown in Supplementary **Table S1**.

3.5.1 Normalization Accuracy

To subjectively illustrate how well each algorithm performed, **Figure 3.2** shows raw T1w images (without lesion-filling) and the corresponding spatially-normalized images following linear (affine), MRIStudio (LDDMM), FSL (FNIRT), ANTs (SyN), and SPM (CAT12) normalization for three representative participants with MS.

Figure 3.2: Corresponding spatially-normalized images of 3 participants from each algorithm

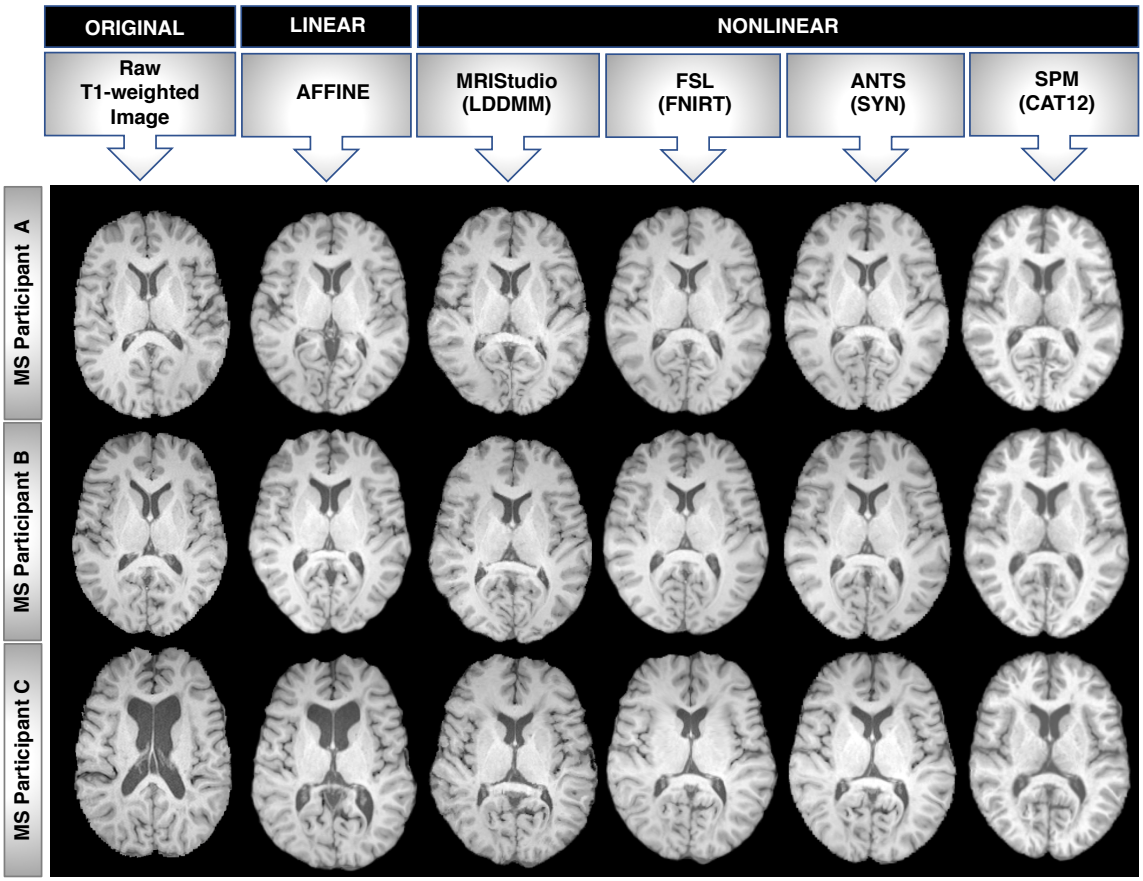

Figure 3.2: T1w images (without lesion-filling), along with the corresponding spatially normalized images using linear (affine), MRIStudio nonlinear (LDDMM), FSL nonlinear (FNIRT), ANTs nonlinear (SyN), and SPM nonlinear (CAT12) algorithms for three randomly-selected participants with MS chosen to highlight how heterogeneous white matter pathology can be, including: Participant A) a large left posterior white matter lesion, Participant B) a small right anterior lesion, and Participant C) substantial white matter atrophy and bilateral anterior lesions. Note: Axial brain images are displayed in neurological convention (left=left); all four nonlinear normalization approaches clearly outperform linear normalization for aligning subcortical structures, including white matter.

The MI analysis (**Figure 3.3a-d**) revealed that nonlinear spatial normalization methods consistently outperformed simple linear (affine) normalization in terms of their ability to produce significantly more consistent spatially normalized images across our sample of participants with MS (**Figure 3.3a and Figure 3.3b**). However, among the nonlinear approaches, SPM (CAT12) yielded the greatest inter-subject correspondence (highest MI values) for both the MS participant dataset (**Figure 3.3a and Figure 3.3b**) and the simulated lesion dataset (**Figure 3.3c and Figure 3d**), whereas FSL (FNIRT) yielded the lowest inter-subject correspondence (lowest MI values). Linear (affine) and MRIStudio (LDDMM) both showed a statistically significant dependence in terms of whether images were lesion-filled or not (**Figure 3.3a**), but these effects were small compared to the differences between the five normalization algorithms for the MS participant dataset. Nonetheless, all five normalization approaches did show significantly higher MI scores as a result of lesion-filling in the simulated lesion dataset (**Figure 3.3c**).

Figure 3.3 a-d: Box-Whisker plots of mutual information (MI) values from each normalization method

a)

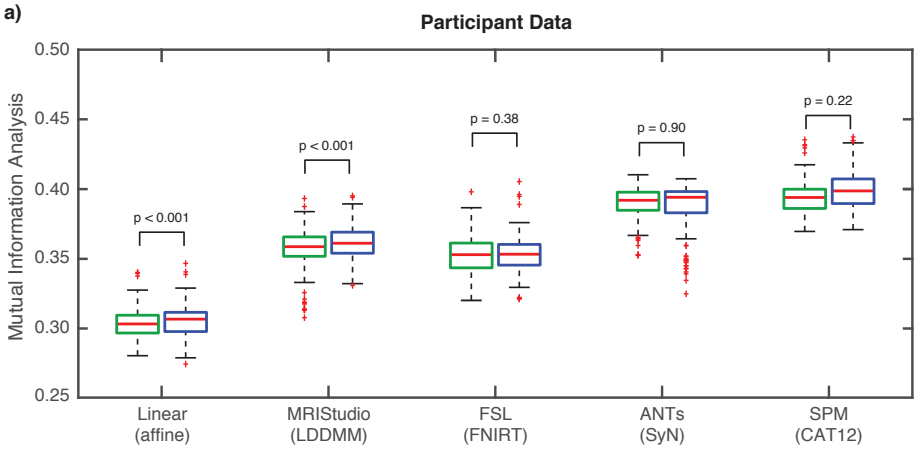

b)

MRIStudio (LDDMM)	$p = 2.00 \times 10^{-221}$			
FSL (FNIRT)	$p = 5.73 \times 10^{-258}$	$p = 1.88 \times 10^{-12}$		
ANTs (SyN)	$p = 7.41 \times 10^{-211}$	$p = 3.92 \times 10^{-67}$	$p = 6.21 \times 10^{-88}$	
SPM (CAT12)	$p = 3.04 \times 10^{-215}$	$p = 2.24 \times 10^{-82}$	$p = 3.89 \times 10^{-112}$	$p = 8.19 \times 10^{-21}$
	Linear (affine)	MRIStudio (LDDMM)	FSL (FNIRT)	ANTs (SyN)

c)

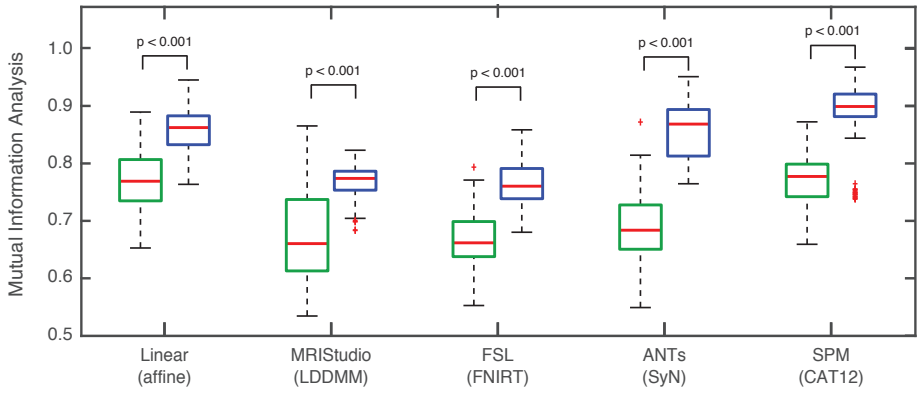

d)

MRIStudio (LDDMM)	$p = 1.55 \times 10^{-116}$			
FSL (FNIRT)	$p = 9.85 \times 10^{-120}$	$p = 0.04$		
ANTs (SyN)	$p = 7.84 \times 10^{-27}$	$p = 9.43 \times 10^{-36}$	$p = 1.54 \times 10^{-44}$	
SPM (CAT12)	$p = 9.23 \times 10^{-09}$	$p = 1.96 \times 10^{-144}$	$p = 1.22 \times 10^{-153}$	$p = 1.48 \times 10^{-69}$
	Linear (affine)	MRIStudio (LDDMM)	FSL (FNIRT)	ANTs (SyN)

Figure 3.3a-d: Box-Whisker plots of mutual information (MI) values based on images from each normalization approach before and after lesion-filling: a) participant data, c) simulated data with p-values indicating within-algorithm differences before vs. after lesion-filling. Corresponding p-values of between-algorithm differences are presented in (b, d). Note: green boxes = non lesion-filled data; blue boxes = lesion-filled data, shaded cells in 2b and 2d indicate p-values ≤ 0.05 (Bonferroni corrected).

Figure 3.4 shows the COV maps and whole-brain COV values for the MS participant and simulated lesion datasets, which highlights inter-subject differences for each spatial normalization pipeline. For the MS participant data (**Figure 3.4a**), and consistent with the MI results, the average COVs for all nonlinear normalization methods were lower than linear normalization. This was particularly evident in periventricular regions, highlighting how ventricular size and shape differences between participants are not well accounted for by simple linear scaling. Among the nonlinear normalization approaches, the SPM (CAT12) algorithm produced the lowest average COV (**Figure 3.4a**), reflecting the least anatomical variability between spatially-normalized participant images. Lesion-filling improved normalization accuracy for all five approaches but these improvements within each algorithm were small in comparison to the relatively large COV differences between algorithms. Conversely, for the simulated lesion dataset (**Figure 3.4b**), linear (affine) normalization showed the least variability between normalized images. Similar to the results obtained in the MS participant data and the results based on MI values, the SPM (CAT12) algorithm produced the best results in terms of lowest COV values among the nonlinear normalization approaches. Lesion-filling again improved normalization accuracy for all five approaches, and these improvements were larger than those observed in the MS participant dataset.

Figure 3.4 a-b: Coefficient of Variation maps for each spatial normalization method

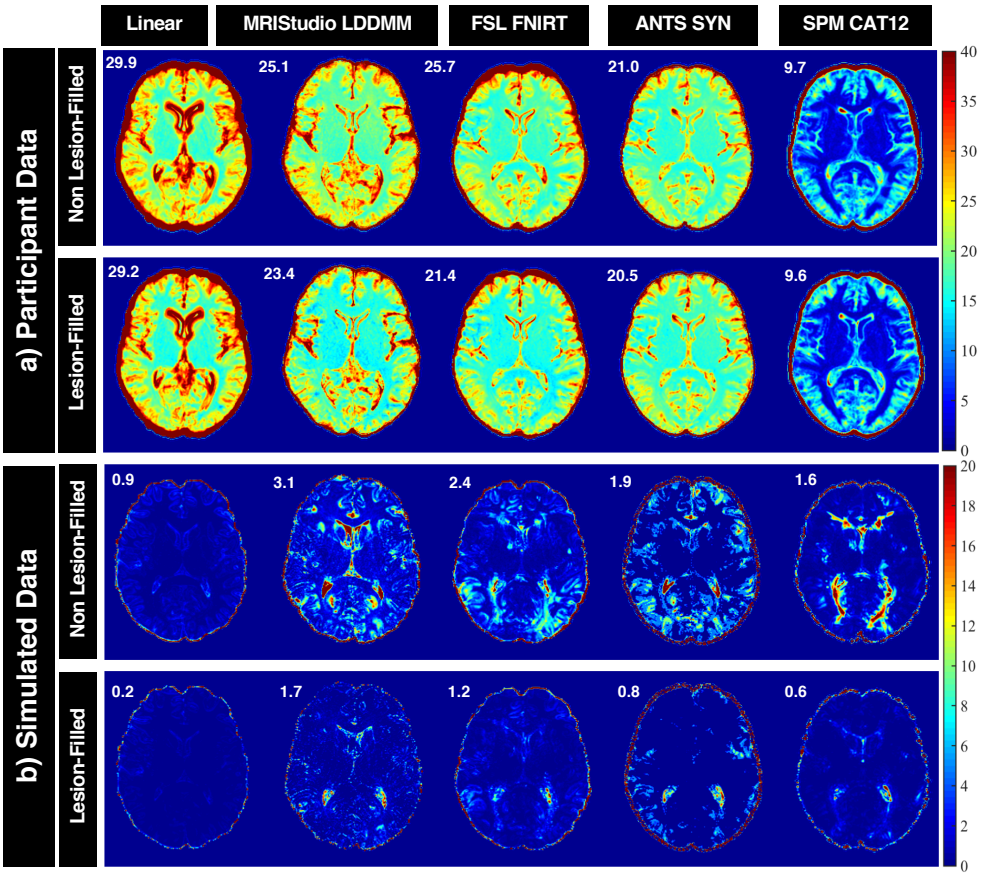

Figure 3.4 a-b: Between-participant coefficient of variation (COV) maps based on each normalization approach before and after lesion-filling: a) participant data and b) simulated data. Whole-brain average COV values are shown for each approach, where higher COV values indicate greater between-participant variability.

3.5.2 Normalized Lesion Volumes

Figure 3.5 shows the lesion volumes before and after spatial normalization with each method. Given that the MNI brain template is slightly larger than most typical adult brains, lesion volumes increased as a result of spatial normalization to this template with all five methods, both with and without lesion-filling. Based on the MS participant data (Figure 3.5a), average lesion volumes were increased by ~35% for linear (affine), ~60% for MRIStudio (LDDMM), ~100% for FSL (FNIRT), and ~40% for ANT (SyN) and SPM12 (CAT12). Based on paired-sample t-tests, FSL (FNIRT) ($p=0.001$) and ANTs (SyN) ($p=0.003$) were the only normalization approaches to show within-method differences due to lesion-filling. Conversely, significant differences were found for all between-method comparisons (Figure 3.5b) except linear (affine) vs. ANTs (SyN) ($p=0.06$) and SPM (CAT12) vs. ANTs (SyN) ($p=0.28$), indicating that lesion volumes were influenced more by the spatial normalization approach than lesion-filling.

Within the simulated lesion dataset, lesion volumes also increased as a result of spatial normalization and in this case, all approaches showed significant within-method differences due to lesion-filling (**Figure 3.5c**). Paired-sample t-tests also revealed significant differences between all spatial normalization approaches (**Figure 3.5d**) except linear (affine) vs. ANTs (SyN) ($p=0.31$), linear (affine) vs. MRIStudio (LDDMM) ($p=0.67$), and MRIStudio (LDDMM) vs. ANTs (SyN) ($p=0.57$).

Figure 3.5 a-d: Lesion volumes for each normalization method after lesion-filling

a)

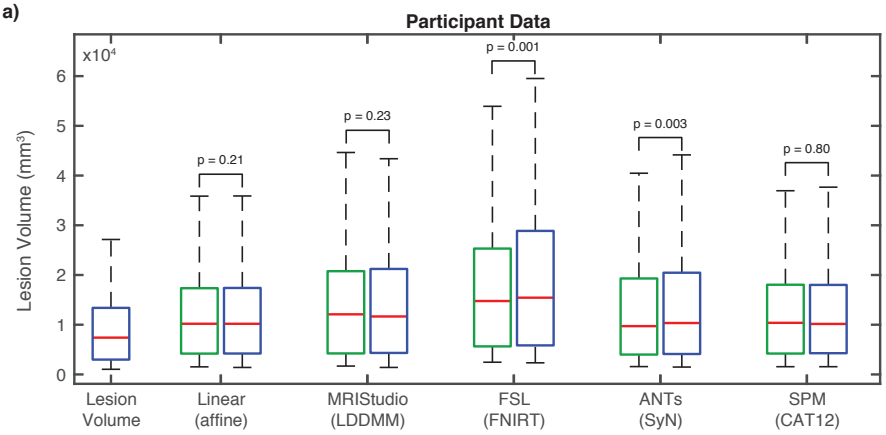

b)

MRIStudio (LDDMM)	p = 7.5 x 10^{-5}			
FSL (FNIRT)	p = 1.17 x 10^{-7}	p = 4.22 x 10^{-7}		
ANTs (SyN)	p = 0.06	p = 7.13 x 10^{-4}	p = 9.09 x 10^{-11}	
SPM (CAT12)	p = 4.51 x 10^{-3}	p = 7.13 x 10^{-5}	p = 3.14 x 10^{-8}	p = 0.28
	Linear (affine)	MRIStudio (LDDMM)	FSL (FNIRT)	ANTs (SyN)

c)

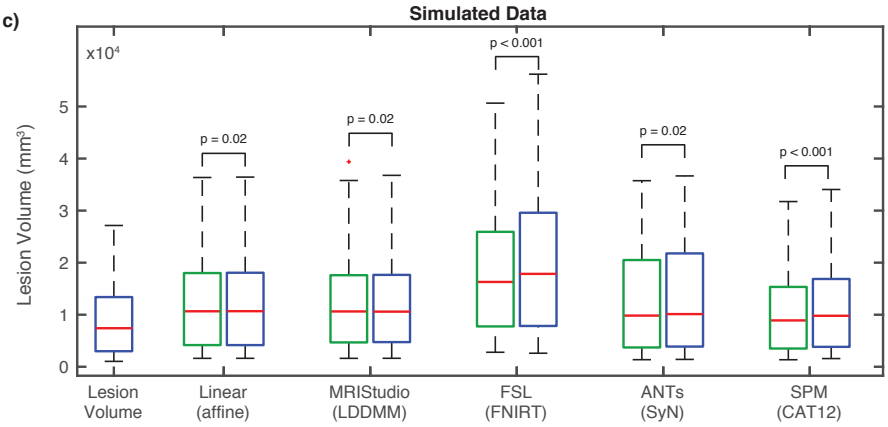

d)

MRIStudio (LDDMM)	p = 0.67			
FSL (FNIRT)	p = 8.71 x 10^{-12}	p = 2.25 x 10^{-11}		
ANTs (SyN)	p = 0.31	p = 0.57	p = 2.18 x 10^{-7}	
SPM (CAT12)	p = 3.90 x 10^{-7}	p = 7.43 x 10^{-5}	p = 1.07 x 10^{-11}	p = 0.01
	Linear (affine)	MRIStudio (LDDMM)	FSL (FNIRT)	ANTs (SyN)

Figure 3.5 a-d: Box-Whisker plots of lesion volumes based on each normalization approach before and after lesion-filling: a) participant data, c) simulated data with p-values indicating within-algorithm differences before vs. after lesion-filling. Corresponding p-values of between-algorithm differences are presented in (b, d). Note: green boxes = non lesion-filled data; blue boxes = lesion-filled data, shaded cells in 4b and 4d indicate p-values ≤ 0.05 (Bonferroni corrected).

3.5.3 Single-Subject Analyses

In our single-subject example using one representative participant with MS, inverse deformations of the JHU-MNI-ss (Eve) Atlas based on each normalization method produced different estimated volumes of the caudate, thalamus, genu and splenium (**Supplementary Figure 1a**). Moreover, the corresponding masks of these regions had subjectively poor spatial overlap (**Supplementary Figure 1b**), which was supported quantitatively by modest DSC values, which ranged between 0.50-0.76 (**Supplementary Figure 1c**).

3.6 Discussion

We systematically compared five of the most commonly used and freely available spatial normalization methods, before and after lesion-filling in the presence of MS pathologies and found that nonlinear warping methods systematically outperformed conventional linear normalization in terms of their ability to consistently warp MS participant images to a common template. In particular, SPM12 (CAT12), closely followed by ANTs (SyN), yielded the most consistent results, with the highest MI and lowest COV values among the five approaches examined. Lesion-filling lead to small but reproducible improvements.

These findings are similar to those of Klein et al. who also found SPM and ANTs to be the highest-ranking nonlinear normalization methods in comparisons based on brain imaging data from neurologically healthy volunteers[85]. However, ours was the first study to systematically compare spatial normalization methods in a MS cohort and to evaluate the effects of MS pathologies, including focal lesions, differences in NAWM and GM volumes and signal intensities, using actual MS participant data. Since the goal of this study was to compare the spatial normalization algorithms themselves, we controlled for differences in preprocessing and postprocessing as much as possible. Moreover, we employed a simulated lesion dataset that

exclusively focused on the effects of WM lesions and had a known ground-truth, where the MI should be one and the COV should be zero, because all of the images were based on the same healthy control participant. Thus, because the only variable was the presence of imposed focal lesions during the spatial normalization step, and the linear normalization is not sensitive to local features, it is not surprising that the linear (affine) normalization showed the least variability between normalized images in the simulated lesion dataset.

Taken together, MI and COV results from the MS participant and simulated lesion dataset provide several important insights into different aspects of MS pathology and how they affect spatial normalization. First, WM lesions alone account for a sizable portion of the inter-subject variability between spatially normalized images. Second, lesion-filling before spatial normalization significantly reduced inter-subject differences related to WM lesions. Third, factors such as brain atrophy and NAWM and GM signal intensities also led to substantial reductions in normalization accuracy. Fourth, these more global differences in tissue volume and signal intensity are affected little by whether or not images are lesion-filled before spatial normalization. Another finding that clearly emerges from our data is that depending on the choice of software and their spatial normalization algorithms, MS WM lesions and other inter-subject differences are accounted for quite differently.

The latter point is particularly important to consider given that in the absence of empirical comparisons to establish optimal methods, researchers tend to rely on techniques with which they are most familiar. Such variations in choice of methods increase the chances of systematic differences occurring in spatial normalizations between individuals or groups. This, in turn, could negatively impact study conclusions in two ways. First, erroneous inter-individual or inter-group differences (type I errors) could potentially emerge from inaccurate spatial normalizations

due to invalid comparisons between different structures or tissue types. Second, sensitivity to true inter-individual or inter-group differences could be obscured (type II errors) due to inconsistently localized effects. Because spatial normalization represents a critical early step in the analysis pipeline, measures should be taken to ensure it is performed optimally.

Although we found that different spatial normalization approaches had significantly different effects on lesion volumes, these differences were small, and our findings confirmed that none of the methods evaluated in our tests severely mishandled focal WM lesions (e.g., by systematically shrinking their volume to zero) even when lesion-filling was not performed. This served as an important quality assurance check within the current study, and also provided an important verification for both previous and future studies of MS and other WM disorders.

Finally, the results of our single subject example highlight how different spatial normalization methods can produce very different volume estimates for individual brain structures. Moreover, the maps of spatial overlap, and the DSC calculations show that the shapes (3D locations) of the atlas-based brain parcellations are also quite different, falling below previously established thresholds of DSC > 0.7 for 'good' agreement between the resulting segmentations[113]. Therefore, in addition to affecting deformation-based volumetric estimates, the choice of spatial normalization algorithm will substantially affect neuroimaging-based comparisons between individuals and groups.

3.7 Study Limitations

This study has some notable limitations. First, we investigated only five of the available spatial normalization approaches for brain MRI data. These particular approaches were chosen because an exhaustive comparison between all available methods was not feasible, and these five are among the most common spatial normalization approaches used in contemporary

neuroimaging studies. Moreover, all five algorithms are included in software packages that are freely available. However, it is possible that another existing method would have out-performed the algorithms currently tested. Second, and also for feasibility-related reasons, each spatial normalization approach was only tested using the default parameters within its respective software package (unless otherwise noted), although some of the methods have several modifiable parameters. The rationale for this was that the developers of each algorithm set the default parameters based on internal testing and optimization; and because most researchers use these default settings, this likely provided the most common real-world set-up for each software package. Nonetheless, future studies could conduct further testing with different internal parameters (e.g., spatial resolution, smoothing, etc.) to further refine spatial normalization accuracy and overall pipeline performance. Third, only one lesion-filling approach was tested. Given that the primary focus of the study was on spatial normalization algorithms, a detailed comparison between different lesion-filling approaches was beyond the scope of the current study. Our testing showed relatively modest differences depending on whether images were lesion-filled or not compared to the larger differences based on which software package and normalization algorithm was used. Nonetheless, our results may have differed somewhat if we had used other lesion-filling approaches and this could be examined in future work focused on that topic. Fourth, because multiple software packages were used and each one comes with its own MNI template that includes different image dimensions and spatial resolutions, we first resampled each template to 1.0 mm cubic resolution when necessary in order to eliminate this as a variable between methods. However, for FSL (FNIRT) and SPM (CAT12), we also re-ran all of the spatial normalizations using their default templates (2.0 mm and 1.5 mm cubic resolutions,

respectively), and neither the resulting COV maps nor the resulting lesion volumes differed substantively from the results obtained from the higher resolution normalizations.

3.8 Conclusions

Our findings indicate that nonlinear warping methods systematically outperformed linear (affine) spatial normalizations and that the SPM (CAT12) algorithm proved to be the most robust among the methods tested, particularly when using lesion-filled images. We therefore suggest that future MS brain imaging studies use SPM (CAT12) and lesion-filling for optimal spatial normalizations. This should yield more accurate voxel-wise and ROI-based comparisons between MS individuals or groups within each study, and the adoption of a uniform image processing pipeline will allow for more accurate comparisons between studies and facilitate future meta-analyses.

3.9 Acknowledgements

This work was supported by the Waugh Family Foundation Multiple Sclerosis Society of Canada operating grant (EGID-2639), The Canadian Institutes of Health Research (THC-135234), The Winnipeg Health Sciences Centre Foundation (HSCF), The Natural Sciences and Engineering Research Council of Canada (NSERC), and the Brain Canada Foundation. RAM also receives support through a Manitoba Research Chair, as well as a Waugh Family Multiple Sclerosis Research Chair.

3.10 Figure Captions

Figure 3.1: *Comprehensive image-processing pipeline for warping the T1w MRI images and lesion masks from each participant to the Montreal Neurological Institute (MNI) brain template. Spatial normalizations were performed using five commonly used algorithms, both before and after lesion-filling the T1w images. Note: Axial brain images are displayed in neurological convention (left=left); NAWM: normal appearing white matter, LST: lesion segmentation toolbox, LGA: lesion growth algorithm, Non-LF: non lesion-filled, LF: lesion-filled.*

Figure 3.2*: T1w images (without lesion-filling), along with the corresponding spatially normalized images using linear (affine), MRIStudio nonlinear (LDDMM), FSL nonlinear (FNIRT), ANTs nonlinear (SyN), and SPM nonlinear (CAT12) algorithms for three randomly-selected participants with MS chosen to highlight how heterogeneous white matter pathology can be, including: Participant A) a large left posterior white matter lesion, Participant B) a small right anterior lesion, and Participant C) substantial white matter atrophy and bilateral anterior lesions. Note: Axial brain images are displayed in neurological convention (left=left); all four nonlinear normalization approaches clearly outperform linear normalization for aligning subcortical structures, including white matter.*

Figure 3.3: *Box-Whisker plots of mutual information (MI) values based on images from each normalization approach before and after lesion-filling: a) participant data, c) simulated data with p-values indicating within-algorithm differences before vs. after lesion-filling. Corresponding p-values of between-algorithm differences are presented in (b, d). Note: green boxes = non lesion-filled data; blue boxes = lesion-filled data, shaded cells in 2b and 2d indicate p-values* ≤ 0.05 *(Bonferroni corrected).*

Figure 3.4: *Between-participant coefficient of variation (COV) maps based on each normalization approach before and after lesion-filling: a) participant data and b) simulated data. Whole-brain average COV values are shown for each approach, where higher COV values indicate greater between-participant variability.*

Figure 3.5: *Box-Whisker plots of lesion volumes based on each normalization approach before and after lesion-filling: a) participant data, c) simulated data with p-values indicating within-algorithm differences before vs. after lesion-filling. Corresponding p-values of between-algorithm differences are presented in (b, d). Note: green boxes = non lesion-filled data; blue boxes = lesion-filled data, shaded cells in 4b and 4d indicate p-values ≤ 0.05 (Bonferroni corrected).*

Figure S1: *ROI volume estimates of two deep GM structures (caudate and thalamus) and two deep WM structures (genu and splenium of the corpus callosum) based on each normalization approach for a single participant with MS (a), along with subject-space masks of the four regions overlaid for the two most similar normalization approaches (b) and dice similarity coefficient (DSC) values of spatial overlap between all methods.*

Table S1*: Spatial normalization processing times for each participant.*

Chapter 4: Network-based measures of white matter microstructure reflect individual differences in executive function among persons with MS

Running Title: Network-based MRI measures of executive function in MS

Abstract Word Count: 410

Manuscript Word Count: 5431 (excluding the Abstract, Table/Figure Captions and References)

Number of Primary Tables and Figures: 5 Tables; 1 Figure

Number of Supplementary Materials: 0 Supplementary Figures and 0 Supplementary Tables

Keywords: Multiple Sclerosis; MRI; WM; GM; NAWM; DTI; MD; FA; Structural; Functional; Connectivity; Executive Function; DMN; ECN; DKEFS; CWIT;

4.1 Abstract

Background: Prior studies in MS have shown relationships between cognitive performance and resting-state functional connectivity in distributed, large-scale brain networks – specifically the executive control and default mode networks (ECN and DMN). The DMN is a highly consistent cognition-related cortical network involving several brain regions which supports the default-mode activity of the human brain. However, relationships between cognition, particularly executive function (EF), and white matter structural connectivity underlying these networks remain poorly understood.

Objectives: We aimed to use recently released functionally-defined white matter atlases to investigate relationships between EF and tissue microstructure throughout ECN and DMN white matter in an MS cohort. Our *priori* hypothesis was that white matter microstructure in these networks would be positively correlated with EF.

Methods: We obtained 3 Tesla high angular resolution diffusion imaging (HARDI), cognitive test scores and baseline demographic data from 103 MS participants enrolled in the Comorbidity, Cognition and Multiple Sclerosis (CCOMS) Study. White matter integrity was assessed using HARDI-based mean diffusivity (MD) and fractional anisotropy (FA) values extracted from ECN and DMN regions via the UManitoba-JHU Functionally-Defined Human White Matter Atlases. EF was assessed using the Delis-Kaplan Executive Function System Color-Word Interference Test (DKEFS CWIT). One-tailed Spearman partial correlations were performed between ECN and DMN white matter microstructural metrics vs. EF; correcting for age, sex, and premorbid cognitive ability using the Wechsler Test of Adult Reading (WTAR). Post-hoc tests were then performed, using MD values from each participant's global white matter mask, to determine whether (and to what extent) the network-based white matter analyses were more predictive of EF.

Results: EF scores were significantly correlated with individual differences in white matter MD measurements obtained from both the ECN (rho = 0.192; 95% CI = 0.029 to 0.345; p = 0.029) and DMN (rho = 0.194; 95% CI = 0.031 to 0.347; p = 0.027), but not those obtained from global white matter (rho = 0.106; 95% CI = -0.059 to 0.266; p = 0.147) after correcting for age, sex and WTAR. None of the FA values (extracted from either the DMN or ECN) yielded statistically significant correlations with EF after correcting for age, sex and WTAR.

Conclusions: Within our MS cohort, reduced executive functioning was associated with increased MD (decreased microstructure) throughout ECN and DMN white matter networks, but not with global white matter MD measures. These findings indicate that network-based analytic approaches are valuable for studying how participant-specific measures of white matter damage correspond to symptomatic variability among persons with MS.

4.2 Introduction:

Multiple sclerosis (MS) is a chronic inflammatory disease, characterized by multifocal, demyelinated white matter (WM) lesions, and diffuse WM damage throughout normal appearing WM (NAWM)[17,114]. The widespread and variable spatial distribution of these lesions throughout the central nervous system (CNS) results in a range of commonly experienced clinical symptoms; some of which include motor, sensory, visual and cognitive deficits[115]. Cognitive deficits in particular affect about 40-70% of MS patients, with about 15-20% having deficits in higher order executive functions (EF) - rendering it difficult to perform normal daily activities and maintain social functioning[116,117,118]. This is largely due to EF impairments affecting planning, reasoning, problem solving, decision making, multitasking, working memory, and inhibition to list a few – all of which are essential for normal daily functioning. As a result, deficits in EF are among the most frequently reported and the most disabling[119,120]. This has been supported extensively in the literature, whereby numerous studies have found MS patients to have systematically lower EF performance than healthy controls. In addition, some brain imaging studies have found general MRI measures, such as WM hyperintensity volume, to be associated with cognitive impairment, and in particular lower EF and episodic memory[121]; while other studies have reported associations between EF and more localized MRI measures in frontal subcortical WM tracts involving anterior thalamic radiation[74]. Nonetheless, while it is generally agreed that structural damage in MS is linked to cognitive performance, reliable associations between MRI measures and specific types and severities of clinical deficits have remained elusive. In fact, the relatively weak correlations between traditional MRI markers (e.g., number of lesions and lesion volume) and the severity of specific clinical deficits like EF – not to mention limited prognostic value for future decline – at the individual level has been dubbed the clinic radiological paradox[30,40,41,122].

That said, it is not to say that progress has not been made in identifying potential structural MRI correlates of cognition and EF in MS. One study looking at cognitive function (broadly defined) found significant MRI differences between MS patients with and without cognitive impairment[123]. Another recent study has even reported associations between structure and longitudinal cognitive decline, but was only able to achieve this by relying on complex, multivariate statistical models that combined several MRI measures, including regional brain volumes and microstructural measures[124]. Other studies using graph theoretical approaches have also successfully identified structural MRI changes associated with cognitive performance in MS[115]. However, no studies to date have identified a clear neural correlate of EF dysfunction in MS using a single structural MRI measure.

Extensive work has however been done over the past decade using functional MRI (fMRI), which has revealed that the human brain is organized into large-scale functional networks that subserve different mental processes, and that many of these networks appear to be altered by MS[125]. Some studies have found strong associations between network-based functional connectivity in the default mode network (DMN) and executive control network (ECN) and specific markers of cognitive performance and EF[125]. There has also been evidence of altered functional connectivity in deep GM regions and within-network coherence decreases in MS[126]. Evidence has also been presented with altered resting-state fMRI connectivity patterns compared to healthy controls in the visual network (VN), sensorimotor network (SMN) and DMN[127]. Interestingly, functionally-defined WM atlases have recently been created and made freely-available for many of these same networks, including the DMN and ECN– allowing network-based structural MRI measures to be easily quantified and investigated[77,128].

Therefore, the goal of the present study was to use a large and representative MS cohort to investigate the relationships between EF and WM microstructure using a network-based approach in the DMN and the ECN. We anticipate that this network-based approach will be sensitive to individual differences in EF and in turn, lead to the identification of a single structural MRI correlate of EF impairment in MS. In particular, we hypothesize that there will be a positive association between EF impairment and structural connectivity in the DMN and ECN networks, whereby participants with higher EF will have lower MD values and higher FA values, such that lower microstructural integrity will be associated with poorer cognitive performance.

4.3 Methods

4.3.1 Study Participants

This study protocol has been approved by The University of Manitoba Health Research Ethics Board (HREB). Prior to enrollment, written consent was provided by all 111 participants involved in this study. Participants with definite MS were recruited through the Winnipeg Health Sciences Centre MS Clinic and had been previously diagnosed by a neurologist based on the revised McDonald criteria[39]. Of the 111 participants recruited, 93 of them had relapsing remitting MS (RRMS), 12 had secondary progressive MS (SPMS), and 6 had primary progressive MS (PPMS). Study inclusion criteria required all participants to be 18 years or older, provide written informed consent, have adequate knowledge of the English language to complete the study protocol, have adequate sensorimotor function to complete the cognitive tests, have no comorbid brain tumors or neurodegenerative diseases, and a stable course of disease (i.e., with no relapses) and disease modifying therapies (DMTs) for a minimum of 30 days prior to study enrollment. Study exclusion criteria included contraindications to MRI, such as pacemakers,

metallic implants, pregnancy and claustrophobia. Participant characteristics can be found in **Table 4.1.**

4.3.2 Clinical assessments

Neuropsychological testing was performed according to standardized instructions by research coordinators and under the supervision of a single clinical neuropsychologist at the Health Sciences Centre in Winnipeg, Manitoba. Although a wide range of neuropsychological tests were administered as a part of the broader Comorbidity, Cognition and Multiple Sclerosis (CCOMS) study protocol, for the purposes of this study, EF was assessed using the Delis-Kaplan Executive Function System (DKEFS) Color-Word Interference Test (CWIT) and participant pre-morbid IQ was estimated using the Wechsler Test of Adult Reading (WTAR).

4.3.2.1 Executive Function System (DKEFS) Color-Word Interference Test (CWIT)

The DKEFS battery is made up of nine tests, which include the Trail Making, Verbal Fluency, Design Fluency, CWIT, Card Sorting, 20 Questions, Word Context, Tower Test and Proverbs[70]. All nine tests provide 20 primary scores. The DKEFS battery as whole uses standardized versions of several currently used tests to assess a range of executive functions in adults and children aged 8-89 years old[70]. Many of the tests, that have been expanded on from established executive functioning tasks are now more sensitive to subtle changes in cognitive functioning. Though the DKEFS has been deemed to be a robust measure of EF in MS, it has also been well suited in assessing EF impairment in other clinical patient populations such as Parkinson's disease[129], unilateral brain damage[130], Korsakoff syndrome[131] and schizophrenia[73] to list a few.

The present study used scores obtained from the DKEFS CWIT. This test in particular has been designed around the classic Stroop test, which works to measure the ability to inhibit a

dominant and automatic response to provide a more intentional response - ultimately assessing verbal inhibition. However, the CWIT's inhibition/switching trial is unique to the DKEFS version of the Stroop task, and was added to also assess higher order abilities of set switching. The CWIT test works such that, for half of the items in the inhibition/switching task, participants are instructed to name the color of the ink the words are printed in. A rule change is instituted for the other half of the items that requires participants to instead read the actual word, therefore requiring participants to switch back and forth between the automatic response and the intentional response while keeping track of the rule changes. Scores are given based on the total completion time for a fixed number of trials, so that (all else being equal) higher scores indicate lower EF[132]. However, to control for individual differences in basic information processing speed and focus more exclusively on the higher-level inhibition and switching components, each participant's EF was defined in this study as the contrast between the CWIT inhibition/switching task vs. the average of the baseline color naming (Condition 1: where participants name the colors of ink swatches as quickly as possible) and word reading (Condition 2: where participants read color names printed in black and white as quickly as possible) tasks[133].

4.3.2.2 Wechsler Test of Adult Reading (WTAR)

The Wechsler Test of Adult Reading (WTAR) is a neuropsychological test that relies on mental abilities that are thought to remain largely unaffected following many types of neurological damage, and is often used to estimate pre-morbid Wechsler Adult Intelligence Scale IQ and Wechsler Memory Scale index scores. The format of this test requires participants to read 50 words out loud that are presented to them on a card. Their scores from their test are then converted into estimates of pre-morbid IQ/memory, which can then be corrected for (along with other factors such as age and sex) in subsequent statistical analyses.

4.4 Functionally-Defined White Matter Atlases

Although several studies have looked at fMRI vs. cognition relationships in large scale functional networks, the present study worked to overcome gaps in the literature by investigating structural connectivity vs. EF relationships in these same networks. To do so, this study made use of the recently released functionally-defined probabilistic WM atlases (https://www.nitrc.org/search/?type_of_search=group&q=UManitoba-JHU+Functionally-Defined+Human+White+Matter+Atlas), to measure WM signals in regions that are thought to underlie specific networks associated with cognitive and executive domains: namely the dorsal and ventral default mode networks (dDMN, vDMN), and the left and right executive control networks (lENC, rENC)[77]. For the purposes of this study, these will be used to conduct subsequent region of interest (ROI) MRI analyses (described below) to examine the relationships between structural connectivity and cognition within specific networks pertaining to EF in MS.

4.5 Magnetic Resonance Imaging (MRI)

4.5.1 Data Acquisition

Brain imaging data used in this study were acquired using a 3T Siemens TIM Trio MRI system (software version VB17a) equipped with a Siemens TQ-Engine gradient set and a Siemens 32-channel receive-only head coil *(Siemens Healthcare, Erlangen, Germany)*. For each participant, their MRI session included a T1-weighted (T1w), T2-weighted fluid attenuated inversion recovery (T2-FLAIR), and high angular resolution diffusion imaging (HARDI) sequences.

4.5.2 T1w Anatomical Scans

Whole-brain T1w images were acquired using a 3D magnetization prepared rapid acquisition gradient-echo (MPRAGE) sequence with the following parameters: repetition time

[TR] = 1900 ms, echo time [TE] = 3.46 ms, inversion time [TI] = 900 ms, flip angle = 9˚, GRAPPA = 2, matrix size = 256 × 256, Field of View [FOV] = 250 × 250 mm2, number of slices = 176, slice thickness = 0.98 mm, band width [BW] = 170 Hz/Px, echo spacing [ESP] = 8.4 ms, reconstructed spatial resolution = 1.0 × 1.0 × 1.0 mm3, acquisition time [TA] = 4.26 min.

4.5.3 Fluid Attenuated Inversion Recovery (FLAIR) Scans

T2-weighted (T2w) images with water suppression were acquired with an axial 2D Fluid Attenuated Inversion Recovery (FLAIR) turbo spin-echo sequence with the following parameters: TR = 9000 ms, TE = 100 ms, TI = 2499 ms, flip angle = 90˚, refocusing angle = 130˚, matrix size = 256 × 256, FOV = 240 × 240 mm2, number of slices = 32, slice thickness = 4.00 mm, BW = 287 Hz/Px, ESP = 7.17 ms, turbo factor = 16, BW= 287 Hz/Px, number of averages = 1, spatial resolution = 0.94 × 0.94 × 4.00 mm3, TA = 5.06 min.

4.5.4 High Angular Resolution Diffusion Imaging (HARDI) Scans

Fifty non-collinear diffusion-encoded (b=1500 s/mm^2) and five uniformly-interleaved reference (b=0 s/mm2) images were acquired with an optimized q-space sampling scheme[134];http://www.emmanuelcaruyer.com/q-space-sampling.php) and the Human Connectome Project multi-band echo planar imaging (MB-EPI) “cmrr_mbep2d_diff” sequence developed at the Center for Magnetic Resonance Research[135,136]; Release R016 for VB17A, University of Minnesota, (https://www.cmrr.umn.edu/multiband). The following were imaging parameters for this spin-echo MB-EPI sequence: TR = 3284 ms, TE = 89.4 ms, flip angle = 90°, refocusing angle = 177°, matrix size = 106 × 102, FOV = 212 × 204 mm2, number of slices = 80, slice thickness = 2.00 mm, MB factor = 4, number of averages = 1, BW = 1814 Hz/Px, ESP = 0.69 ms, phase partial Fourier = 6/8, spatial resolution = 2.00 × 2.00 × 2.00 mm3, TA = 6:34

min. However, this sequence was acquired twice, with opposite phase encoding directions – i.e., anterior-posterior (AP) and then posterior-anterior (PA) – for a total of 100 diffusion-weighted images (b=1500 s/mm2), 10 reference images (b=0 s/mm2), and an overall TA = 13:08 min.

4.5.5 Data Processing

In terms of HARDI data processing, all diffusion-weighted data were preprocessed using the Artifact Correction In Diffusion MRI (ACID) Toolbox in SPM12 (version 63cc617;http://www.diffusiontools.com), which included both simultaneous motion and eddy current correction. This was based on whole-brain affine registrations[137]. EPI distortion correction was based on the oppositely phase-encoded (blip-up/blip-down) diffusion images and the Hyperelastic Susceptibility artifact Correction (HySCo) algorithm[138]. Whole-brain FA and MD maps were generated using the Fit Diffusion Tensor module and the robust weighted least-squares fitting algorithm to automatically down-weight potential remaining outliers in the diffusion signal[139]. These maps were first coregistered to the MPRAGE image, and later had the overall deformation field using the CAT12 Toolbox applied to them, as shown to be optimal in Chapter 3.

4.5.6 Region of Interest Analyses

A region of interest (ROI) analysis was performed to better understand the relationships between structural connectivity and cognition within specific networks pertaining to EF in MS. To do so, we first spatially normalized each participant's MD and FA maps to the MNI template using SPM CAT12 – the optimal method for spatial normalization in the presence of MS lesions, as identified in Chapter 3. For each participant, we used ROIEditor within MRIStudio to extract MD and FA values from the dDMN, vDMN, lECN, and rECN regions included in the UManitoba-JHU Functionally-Defined Human WM Atlas, and then calculated the average DMN

and ECN values (by taking the average between the dDMN and vDMN sub-networks and the average between the lENC and rECN sub-networks, respectively).

4.6 Quality Assurance and Outlier Rejection

Prior to performing any statistical tests, we first subjected our data to a number of quality assurance checks. Of the 111 participants, 7 were excluded from this study due to diffusion acquisition errors and therefore corrupted images. One additional participant was further excluded due to an outlier in the neuropsychological data. To do so we searched the remaining DKEFS CWIT scores for outliers in MATLAB using the built-in 'rmoutliers' function with default values to remove any participants with a CWIT inhibition/switching contrast greater than 3 standard deviations from the mean. This resulted in the removal of one additional participant, bringing the number of remaining participants to 103.

4.7 Statistical Analyses

The primary measures of interest in this study were each participant's EF score (defined as the contrast between the DKEFS inhibition/switching task vs. the average of the baseline color naming and word reading tasks), MD values from the DMN and ECN, FA values from the DMN and ECN; and covariates to be used as regressors which included each participant's age, sex and WTAR score. Two-tailed conventional Spearman correlations were first performed to characterize the dataset and determine the extent to which each of the continuous variables were correlated; and because sex is a discrete variable, two-tailed Mann-Whitney U-Tests were performed to assess whether any of the continuous variables showed any categorical sex differences.

Then, because we had *a priori* directional hypotheses regarding the MD vs. EF and FA vs. EF relationships, we conducted one-tailed Spearman partial correlations in MATLAB using

the built in 'partialcorr' function to assess relations between the DMN and ECN WM microstructural measures and individual differences in EF, correcting for age, sex and WTAR scores.

4.8 Post-Hoc Analysis

Following the initial DMN and ECN analyses, post-hoc tests were then performed to evaluate whether, and to what extent, the use of this network-based WM approach yielded greater sensitivity to differences in EF than would have been found using a more global MRI measure of WM microstructure. We therefore went back and extracted MD values from the subject-specific global WM masks that were created during the earlier SPM CAT12 spatial normalization. After using ROIEditor in MRIStudio to extract the MD values from each participant's unique WM mask, we then performed one-tailed Spearman partial correlations between these values and EF, correcting for age, sex and WTAR scores. This was therefore analogous in every way to our previous analysis, except that MD values were based on global WM, rather than the network-based ECN and DMN WM segmentations.

We then compared the resulting correlations based on this global post-hoc approach with the correlations based on our initial network-based approach using the Meng test of dependent correlations with overlapping variables[140]. This was done using version 1.1-3 of the freely-available CoCor software package[141] which is available as either a toolbox for the R programing language (https://cran.r-project.org/web/packages/cocor/) or as an interactive web plug-in (http://comparingcorrelations.org/).

4.9 Results

Table 4.1 depicts participant characteristics. **Figure 4.1** depicts the raw DKEFS 4 contrast vs. the raw MD and FA values in each network. These correlations seen in the scatter

plots in **Figure 4.1**, as expected indicate a positive correlation between DKEFS 4 scores and MD values within both the DMN and ECN.

Table 4.1: Participant Characteristics

Participant Characteristics	Mean	SD
Gender of Participants	Females, *n = 83* Males, *n = 19*	
Age	49.05	12.62
WTAR	105.90	10.98
EDSS	3.43	1.49
DKEFS 4	67.15	18.17
DKEFS 4 vs. DKEFS 1 and 2	38.64	14.99
MD Values (DMN)	8.65	0.50
MD Values (ECN)	8.48	0.52
FA Values (DMN)	0.27	0.02
FA Values (ECN)	0.27	0.03

Table 4.1: Participant Characteristics. *Note:* SD = standard deviation, DKEFS 4 = Delis Kaplan Executive Function System Condition 4, DKEFS 1 and 2 = Delis Kaplan Executive Function System Conditions 1 and 2, EDSS: The Expanded Disability Status Scale and WTAR = Wechsler Test of Adult Reading.

Figure 4.1: Straight Correlations

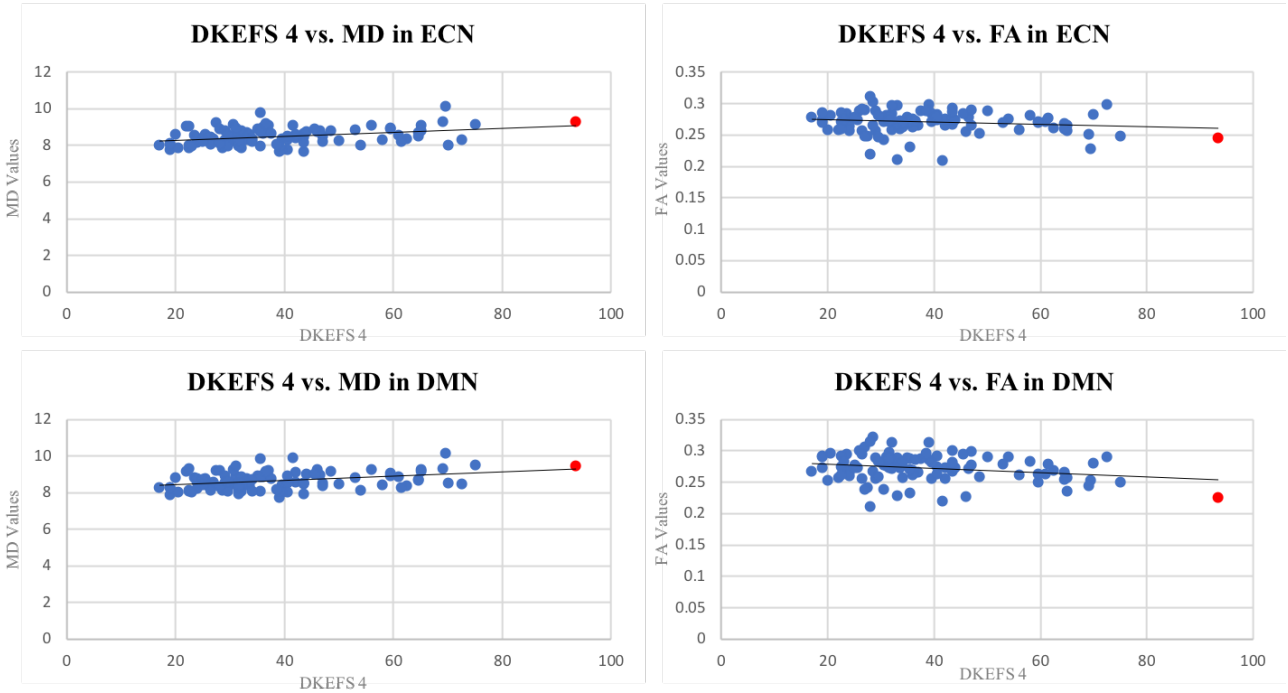

Figure 4.1: Straight correlations were performed as seen in the scatter plots, which indicate a positive correlation between DKEFS 4 scores and MD values in both the DMN and ECN. The red points seen on each scatter plot represent an outlier for which a formal outlier rejection was performed. *Note:* DKEFS 4 = Delis Kaplan Executive Function System Condition 4, MD = Mean Diffusivity, FA = Fractional Anisotropy, DMN = Default Mode Network and ECN = Executive Control Network.

Moreover, values for the one-tailed Spearman partial correlations and the adjusted correlation and its 95% CI can be found in **Table 4.2** The one-tailed Spearman partial correlations suggested that in the DMN, when we contrasted DKEFS 4 vs. MD, we found P_c = 0.0270. Similarly, in the ECN, for DKEFS vs. MD, P_c = 0.0270. Similar trends in contrast, were not found for FA. We first looked at the DMN, where we compared DKEFS vs. FA and found P_c =0.2294. Similarly, in the ECN, for DKEFS vs. FA, P_c =0.5077.

Table 4.2: Spearman Partial Correlations (One-Tailed)

DKEFS4 vs. Imaging metric	Rhoval	95% CI	Pval
DKEFS 4 vs. ECN MD	0.19	0.0289 to 0.3448	0.02
DKEFS 4 vs. DMN MD	0.19	0.0314 to 0.3470	0.02
DKEFS 4 vs. ECN FA	>0.01	-0.1619 to 0.1658	0.50
DKEFS 4 vs. DMN FA	-0.07	-0.2362 to 0.0896	0.22

Table 4.2: Results obtained from performing One-tailed Spearman Partial Correlations, after partialling out the effects of age, sex and WTAR scores. As shown, there were significant partial correlations between executive function and MD values in both the ECN and DMN, but no statistically significant partial correlations between executive function and FA in either network. *Note:* Rhoval = rho-value, 95% CI = 95% confidence interval, Pval = p-value, DKEFS 4 = Delis Kaplan Executive Function System Condition 4, MD = Mean Diffusivity, FA = Fractional Anisotropy, DMN = Default Mode Network and ECN = Executive Control Network.

Conventional direct two-tailed Spearman Correlations, can be seen in **Table 4.3a-c**. When looking at specific networks like the DMN, for MD vs. DKEFS, p=0.0026 and for MD vs. Age, p=0.0017, we found both to be statistically significant. Similarly, when looking at the ECN, similar associations were found with MD. For MD vs. DKEFS, p=0.0019 and for MD vs. Age, p=4.70E-04. However, in both the DMN and ECN networks, MD vs. WTAR did not yield statistically significant correlations.

Table 4.3a. Direct Conventional Spearman Correlations (Two-Tailed)

Network Independent	Rhoval	Pval
Age vs. DKEFS 4	0.28	> 0.01
Age vs. WTAR	0.01	0.88
DKEFS 4 vs. WTAR	-0.21	0.02

Table 4.3b.

DMN Network	Rhoval	Pval
FA vs. DKEFS 4	0.28	> 0.01
FA vs. Age	0.01	0.88
FA vs. WTAR	-0.21	0.02
MD vs. DKEFS 4	0.29	> 0.01
MD vs. Age	0.30	> 0.01
MD vs. WTAR	-0.14	0.13

Table 4.3c.

ECN Network	Rhoval	Pval
FA vs. DKEFS 4	-0.08	0.41
FA vs. Age	-0.18	0.05
FA vs. WTAR	0.13	0.19
MD vs. DKEFS 4	0.30	> 0.01
MD vs. Age	0.34	> 0.01
MD vs. WTAR	-0.15	0.12

Tables 4.3a - 4.3c: Conventional Spearman Correlations (Two-Tailed) were performed after correcting for age, sex and WTAR scores to determine whether any pair of continuous variables were correlated. These results suggest statistically significant relationships between MD values and the two covariates – DKEFS 4 and Age in both networks. In the DMN and ECN networks, MD vs. WTAR did not yield statistically significant correlations. *Note*: Rhoval = rho value, Pval = p-value, DKEFS 4 = Delis Kaplan Executive Function System Condition 4, MD = Mean Diffusivity, FA = Fractional Anisotropy, DMN = Default Mode Network, ECN = Executive Control Network and WTAR = Wechsler Test of Adult Reading.

Using a two-tailed Mann-Whitney U-Test, as seen in **Table 4.4a-c** we compared the independent variable of Sex vs. DKEFS, p=0.83, Sex vs. Age, p=0.26, and Sex vs. WTAR, p=0.86 – all of which were network independent, and found there to be no significant effects

overall and therefore a lack of a Sex effect generally. We then wanted to investigate whether the results would be the same when comparing Sex to FA and MD within the DMN and ECN. Based on this, we found that within the DMN, Sex vs. FA, p=0.98 and Sex vs. MD, p=0.77, was aligned with previous findings – lacking an overall sex effect. Similarly, when investigating the effects of Sex in the ECN, we found similar results; such that Sex vs. FA, p=0.94 and Sex vs. MD, p=0.40 which ultimately also proved to have no statistically significant results. Taken together, the two tailed Mann-Whitney U-Tests indicated that there was a lack of a sex effect.

Table 4.4a. Direct Mann-Whitney U-Tests (Two-Tailed)

Network Independent	Zval	Pval
Sex vs. DKEFS 4	-0.21	0.83
Sex vs. Age	1.10	0.26
Sex vs. WTAR	-0.17	0.86

Table 4.4b.

DMN Network	Zval	Pval
Sex vs. FA	0.01	0.98
Sex vs. MD	-0.28	0.77

Table 4.4c.

ECN Network	Zval	Pval
Sex vs. FA	-0.06	0.94
Sex vs. MD	-0.83	0.40

Tables 4.4a - 4.4c: Mann-Whitney Tests (Two-Tailed) were performed to determine whether any of the continuous variables showed a categorical sex difference. These results indicate that there were no significant effects overall and therefore a lack of a sex effect generally. *Note:* Rhoval = rho value, Pval = p-value, DKEFS 4 = Delis Kaplan Executive Function System Condition 4, MD = Mean Diffusivity, FA = Fractional Anisotropy, DMN = Default Mode Network, ECN = Executive Control Network and WTAR = Wechsler Test of Adult Reading.

4.10 Discussion

This study used a large and representative MS cohort to investigate whether relationships could be identified between EF impairment and microstructure in two functionally defined WM brain networks, namely the DMN and the ECN. As expected, EF scores were significantly correlated with individual differences in WM MD measurements obtained from both networks. The use of recently released functionally-defined WM atlases to investigate this relationship, appeared to be more sensitive to individual differences in EF impairment than corresponding global WM measures. Overall, our findings indicated that these network-based measures represented more straightforward and easily-interpretable structural MRI correlates of EF in MS compared to previous structural MRI studies.

The findings presented in this study on the association between structural connectivity and EF dysfunction suggest a clear association between cognitive impairment (EF impairment in particular) and WM microstructure in the DMN and ECN networks - which also happens to be aligned with much of the functional connectivity literature. For instance, several fMRI studies have investigated the role of the DMN and presented evidence of altered DMN functional connectivity in MS[125,142], although not necessarily in early CIS[143]. Further evidence has also been presented by Bonavita et al., who reported a complex reorganization pattern of the DMN, in relation to cognitive dysfunction[144]. Neuroimaging studies have also supported an association between both DMN and ECN functional connectivity and changes in cognitive status of MS patients[145]. In fact, one study by Roosendaal et al. reported that patients with CIS compared to HCs, showed significantly higher synchronization in the ECN which supports the hypothesis of increased resting state networks functional connectivity changes being a possible compensatory mechanism for widespread brain tissue damage caused by MS[143].

In some studies combining fMRI and DTI, DMN functional connectivity has also been shown to differ between MS and healthy controls, as well as between cognitively impaired and cognitively preserved MS participants; and where functional connectivity in the MS group appeared to correlate with diffusion imaging measures in the corpus callosum and the cingulum WM[146]. Similarly, a study by Hawellek et al., reported that the DMN exhibited increased functional connectivity that was correlated with cognitive ability among MS participants, despite the presence of large and widespread reductions in DTI-based measures throughout the central WM[125]. These studies therefore also tend to support the hypothesis that increased resting state activity and functional connectivity might be a compensatory mechanism for widespread WM damage[147]. However, fMRI studies of MS have tended to investigate cognitive impairment (more broadly defined), rather than focusing in on EF impairment, and even those combining fMRI and diffusion imaging have unfortunately not applied similar network-based analytic approaches to investigate the microstructure of the DMN or other large-scale brain networks.

Previous studies examining associations between specific cognitive domains and structural connectivity, have done so using DTI as a measure of WM integrity in MS. These studies have, however, used different study populations, cognitive testing batteries, and other experimental approaches, which has led to discrepancies and inconsistent findings in the literature. For instance, one study reported an association between reduced FA and impaired performance on a task of planning and organization[50]. One year later, another study then reported contrasting results, since their study failed to find any significant relationships between FA and behavioral performance using a sorting task[69].

More recently, however, there has been more agreement in the literature whereby DTI studies have now begun to report overlapping findings of disrupted structural integrity in various

WM tracts in MS, including the optic radiation, the corpus callosum and the corticospinal tract. However, many of those studies used relatively weaker associations, whereby they correlated FA changes to EDSS scores using a VBM approach[148]. One study that looked at specific functional brain works, similar to this current study was by Shu et al., whereby they used DTI tractography and a sample size of 39, and reported reduced network efficiency in the WM structural networks in MS using graph theoretical measures. Through correlating topological efficiencies with EDSS scores and disease durations, they found pronounced changes in the sensorimotor, visual, DMN and language areas. Despite these findings, in contrast to the present study, that study lacked a clear one-to-one correlation, as they investigated a series of cognitive deficits throughout various networks, rendering it difficult to isolate the effects of EF. Therefore, in contrast to that study, the present study's findings of decreased microstructural integrity (as measured by MD) within both networks being associated with poorer EF performance, which was measured through Condition 4 of the DKEKS CWIT – the most cognitively demanding tasks, allowed us to isolate the effects of EF dysfunction. Together, our large sample size, network-based approach and use of a robust neuropsychological measure to assess EF overcame many of the gaps in the literature. That said, although many of the aforementioned studies had small sample sizes, used 1.5T MRIs, and did not investigate DTI relationships between WM integrity and structural integrity and EF function in MS, one study by Llufriu et al., reported associations between structural networks and FA in attention and EF, assessed with the Paced Auditory Serial Addition Test (PASAT) and Symbol Digit Modality Test (SDMT) – of which attention, auditory, working memory, information processing speed and visual attention could be examined. Their findings were in line with the aforementioned studies in MS, whereby structural brain network is less efficient due to widespread impairment of WM connections and GM structures[117]. In fact, one recent study

published in 2019 found widespread reduction in the structural integrity of the brain network in MS, even in the absence of cognitive decline[149]. Based on these aforementioned studies, it is clear that little is known about the relationship between EF and microstructure throughout the DMN and ECN WM.

Although anatomically-defined WM atlases have been used in many previous studies of MS, ours was the first to use functionally-defined WM atlases to relate structural MRI changes within specific brain networks to a particular clinical deficit. Based on this, to our knowledge, this is the first study to use this set of functionally-defined probabilistic WM atlases to uncover an association between EF impairment and microstructure throughout the DMN and ECN WM. Moreover, one recent study published in 2019, investigated the associations of DMN and CBL-DMN structural connectivity with processing speed in 68 MS patients and 22 HCs, as assessed by the SDMT and mean FA as the weighting factor. Interestingly, this study also employed a network-based approach, which was moderately analogous to this current study's approach to cater to the highly subject-specific cognitive deficits in MS - specifically processing speed. Their network approach, motivated by describing decline of a specific cognitive domain (i.e. processing speed), led to significant findings of the role of the cerebellum structural connectivity to the DMN in information processing speed decline[150]. Their findings however, unlike the present study were based on graph theoretical measures as opposed to performing a straight one-to-one correlation. Nonetheless, their findings, similar to the present study support the notion that MS-related structural alteration affects network functioning, which in turn lends further support to the rationale of the present study. Although their focus was processing speed, and not EF, it is clear that a regionally defined approach can potentially yield more sensitive results.

One study by Genova et al. examined the relationship between EF and DTI-based measures of WM integrity in MS by exploring the association between processing speed and FA. Although there were some similarities between this study and ours, including the use of DKEFS, the two studies are in fact quite different in several important ways. First, Genova et al. used both the DKEFS Trail Making Test (TMT) and the CWIT reporting that performance on both EF tasks (albeit more so for the TMT than the CWIT) were highly dependent on processing speed[74]. However, their sample size was fairly small, including only 25 MS participants and 15 HC's, and the groups were not matched for age, which may be relevant given that Denney et al. reported that age is significantly related to each measure of processing speed[151] and DTI measures (including those in our study) correlate with age. It is also worth noting that the TMT includes a motor component, so it is possible that the larger effect observed in that test could be due to confounded motor deficits. Furthermore, the analysis of their brain imaging data was largely exploratory in nature (i.e., based on a data-driven approach to identify which WM regions exhibited significant correlations between FA and EF). In contrast, our study employed a sample size of 103 MS participants, and the brain imaging data analysis was purely hypothesis driven and based on examining relationships between structural measures throughout two *a priori* functionally-defined WM networks.

As mentioned previously, our study also focused on establishing a neural correlate of EF impairment in particular, something that has been particularly elusive, rather than cognition in general. Therefore, our approach was more focused compared to studies like Yu et al., where they assessed cognitive impairment using the SDMT, Rey Auditory Verbal Learning Test (RAVLT) and PASAT. Their findings, based on 37 MS participants and 20 HC's, suggested that lower FA coupled with higher MD values were significantly correlated with each of the three

cognitive scores in various brain regions identified via group differences compared to HC's, with the strongest associations found with the SDMT – which assesses processing speed and visual working memory[152]. However, while their follow-up analysis to correlate individual differences among MS participants – as opposed to the majority of studies focusing solely on group differences – is conceptually similar to the approach taken in our study and a handful of others, including Tovar-Moll et al., who correlated MD in the thalami of 13 RRMS and 11 SPMS patients with EDSS and PASAT scores[153], ours is the first study to employ functionally-defined WM atlases to perform such correlations. Furthermore, these studies employed numerous neuropsychological measures to assess a wide range of cognitive domains including visual working memory and processing speed to list a few[154], rather than a single test that was specifically chosen to evaluate individual differences in EF dysfunction.

4.11 Study Limitations

Our work is not without limitations. Seeing as how this is a cross-sectional study, the associations presented were not able to grasp EF dysfunction at multiple time points to be able to determine causation. Therefore, future work should involve performing a longitudinal study on the associations of EF dysfunction and microstructure to establish a true cause and effect relationship by observing EF dysfunction over time. By doing so, we can work toward potentially drawing predictive conclusions. Moreover, our sample of MS participants may have influenced our results. The effect of this limitation is that some participants may have had more lesions and in turn greater EF dysfunction than the other participants. Future studies can then work to use a more representative sample using participants with comparable cognitive abilities. Another limitation is the use of diffusion based metrics. The effect of this limitation is that, the present study could not explore myelin specifically and in turn the way it had affected the results

and our interpretation of these results. Therefore, future studies may want to employ MWI techniques to investigate whether it is microstructure driving these EF effects, or if it is myelin specifically. Another limitation is that the present study only looked at two networks, namely the DMN and ECN. To overcome this, future studies can then further explore whether structural connectivity in other functionally-defined brain networks – e.g., the salience network (SN), which is closely associated with both the DMN and ECN– leads to similar associations as presented in this study. Moreover, in the present study, we only found an association with one measure (MD), and not with FA which would have been more in line with some of the functional connectivity work that had been done. Another limitation is that the focus of the present study was EF dysfunction and for that reason a single robust test used to assess EF (DKEFS) was employed. Therefore disability in all cognitive domains were not assessed and further studies may want to use a network-based approach to investigate other cognitive domains in other networks. Furthermore, much of the literature correlated processing speed to that of EF decline, so perhaps taking that into account could have perhaps led to a more extensive assessment of EF.

4.12 Conclusions

Taken together, this study suggests a strong cross sectional association between a single MRI metric related to EF in MS. Specifically, we found that EF impairment was strongly correlated with individual differences in MD values within the DMN and ECN networks. In addition to identifying a possible neural correlate of EF in MS, these promising results potentially pave the way for future longitudinal studies to employ similar network-based analytic approaches to better understand how cognitive processes depend on structural integrity within specific WM pathways, and to determine if these methods could be helpful in predicting future cognitive decline among persons with MS.

4.13 Acknowledgments

This work was supported by the Waugh Family Foundation Multiple Sclerosis Society of Canada operating grant (EGID-2639), The Canadian Institutes of Health Research (THC-135234), The Winnipeg Health Sciences Centre Foundation (HSCF), The Natural Sciences and Engineering Research Council of Canada (NSERC), and the Brain Canada Foundation. RAM also received support through a Manitoba Research Chair, as well as a Waugh Family Multiple Sclerosis Research Chair.

4.14 Figure Captions

Figure 4.1: *Straight correlations were performed as seen in the scatter plots, which indicate a positive correlation between DKEFS 4 scores and MD values in both the DMN and ECN. The red points seen on each scatter plot represent an outlier for which a formal outlier rejection was performed. Note: DKEFS 4 = Delis Kaplan Executive Function System Condition 4, MD = Mean Diffusivity, FA = Fractional Anisotropy, DMN = Default Mode Network and ECN = Executive Control Network.*

Table 4.1: *Participant Characteristics. Note: SD = standard deviation, DKEFS 4 = Delis Kaplan Executive Function System Condition 4, DKEFS 1 and 2 = Delis Kaplan Executive Function System Conditions 1 and 2, EDSS: The Expanded Disability Status Scale and WTAR = Wechsler Test of Adult Reading.*

Table 4.2: *Results obtained from performing One-tailed Spearman Partial Correlations, after partialling out the effects of age, sex and WTAR scores. As shown, there were significant partial correlations between executive function and MD values in both the ECN and DMN, but no statistically significant partial correlations between executive function and FA in either network. Note: Rhoval = rho-value, 95% CI = 95% confidence interval, Pval = p-value, DKEFS 4 = Delis Kaplan Executive Function System Condition 4, MD = Mean Diffusivity, FA = Fractional Anisotropy, DMN = Default Mode Network and ECN = Executive Control Network.*

Table 4.3: *Conventional Spearman Correlations (Two-Tailed) were performed after correcting for age, sex and WTAR scores to determine whether any pair of continuous variables were correlated. These results suggest statistically significant relationships between MD values and the two covariates – DKEFS 4 and Age in both networks. In the DMN and ECN networks, MD*

vs. WTAR did not yield statistically significant correlations. Note: Rhoval = rho value, Pval = p-value, DKEFS 4 = Delis Kaplan Executive Function System Condition 4, MD = Mean Diffusivity, FA = Fractional Anisotropy, DMN = Default Mode Network, ECN = Executive Control Network and WTAR = Wechsler Test of Adult Reading.

Table 4.4: *Mann-Whitney Tests (Two-Tailed) were performed to determine whether any of the continuous variables showed a categorical sex difference. These results indicate that there were no significant effects overall and therefore a lack of a sex effect generally. Note: Rhoval = rho value, Pval = p-value, DKEFS 4 = Delis Kaplan Executive Function System Condition 4, MD = Mean Diffusivity, FA = Fractional Anisotropy, DMN = Default Mode Network, ECN = Executive Control Network and WTAR = Wechsler Test of Adult Reading.*

Chapter 5: Summary

5.1 Discussion

To briefly recap, the purpose of this thesis was to: 1) compare spatial normalization methods on brain MRI data in the presence of MS lesions using real and simulated data to identify an optimal approach for comparing quantitative structural imaging metrics across participants, and 2) use this robust spatial normalization method to investigate the relationships between EF and microstructure throughout the DMN and ECN WM using recently released functionally-defined WM atlases. Together, these two objectives worked to expand our understanding of best-practices in MRI data analysis and the variability in cognitive functioning among persons with MS.

The rationale for investigating the first objective in this thesis was to overcome the absence of an established 'best' practice guideline for spatially normalizing brain imaging data in the presence of MS pathologies. Although studies on spatial normalization algorithms and brain templates have been developed for neurologically healthy adults, no studies have compared spatial normalization methods in the presence of MS-related pathologies [155]. In a similar vein, several studies in the past also worked to compare different image processing pipelines and spatial normalization methods on diseases like Alzheimer's disease, mild cognitive impairment (MCI), drug-resistant epilepsy and stroke[156,157]. Together, this then highlighted the need for identifying an algorithm for MS. Therefore, these findings overcome this gap, by being the first study to compare the performance of five commonly and freely-available spatial normalization approaches to ultimately identify the most robust method for spatially normalizing brain imaging data in the presence of MS lesions. Specifically, this study identified SPM CAT12 as the most robust algorithm for spatially normalizing MS data among the methods tested, particularly when using lesion-filled images. Therefore, my findings suggest that future MS imaging studies (including my subsequent study on structural imaging correlates of EF) should use SPM CAT12

and lesion-filling for optimal spatial normalizations. Taken together, these findings will now enable MS researchers to follow a uniform image processing pipeline for more accurate comparisons.

The rationale for the second objective in this thesis stemmed from existing knowledge about relationships between cognitive performance and resting-state functional connectivity in distributed, large-scale brain networks. Although there is a growing body of literature about functional brain connectivity in MS, no prior study had looked at the relationships between cognition, EF and WM structural connectivity within the ECN or DMN – despite the fact that the WM degeneration is the hallmark of MS pathology. For this reason, the second objective of this thesis worked to build on the first objective, by using SPM CAT12 to generate our FA and MD maps, and to then use these imaging metrics in conjunction with recently released functionally-defined WM atlases to investigate the relationships between cognition, EF and microstructure throughout the DMN and ECN WM. Our findings from this study did in fact show EF to be correlated with individual differences in WM MD measurements obtained from both the DMN and ECN. The implications of these findings are potentially very important, and suggest that network-based imaging measures should be used in future studies combining MRI and cognitive assessments among MS patients (including longitudinal studies of cognitive decline).

5.2 Future Directions

Future work can be done on the findings presented in this study by perhaps using quantitative tract integrity profiles (Q-TIPS) – a novel toolbox created in our lab to estimate further the microstructural integrity and the trajectories of WM pathways. Since Q-TIPS is a toolbox that works to perform tract-based analysis by extracting quantitative MRI data along WM tracts, we could potentially build on the current network-based approach by examining

changes throughout the entire ECN and DMN to ultimately determine whether individual differences in EF can be ascribed to specific WM pathways. It would also be interesting to examine whether structural connectivity in other functionally-defined brain networks – e.g., the salience network (SN), which is closely associated with both the ECN and DMN– using the same functionally defined WM atlases used in this thesis. Based on the significant relationships identified in our study (i.e., between EF in both ECN and DMN structural connectivity), it would be interesting to find SN connectivity related to differences in cognitive deficits in MS. Moreover, this work could also be looked at in sub-networks, such as right vs. left ECN for instance or right vs. left in the DMN – since both the DMN and ECN seemed to correlate positively with DKEFS condition 4 scores. In doing so, as opposed to using DTI imaging metrics, it might be interesting to explore another quantitate MRI imaging measures such as myelin water imaging (MWI) which has been shown to be more a more specific measure of myelin.

Moreover, although this study chose to use condition 4 of the DKEFS CWIT that is thought to measure both task inhibition and switching, future studies could potentially examine sub-domains of EF (e.g., based on condition 3 of the DKEFTS CWIT to investigate task inhibition exclusively, or to perform a contrast between condition 4 and condition 3 of the DKEFS to investigate the switching component, exclusively). It would also be valuable to look at other non DKEFS measures of cognitive function such as cognitive fatigue, which is a major issue itself. Since this thesis did find the network-based approach to be more sensitive than simply using global WM or NAWM values using condition 4, it would be interested to use these findings in the context of looking exclusively at condition 3's inhibition or switching component.

It would also be valuable to conduct some longitudinal studies looking at cognition, EF and structural connectivity patterns to see whether the biomarker identified in this study could have value in predicting future cognitive decline. More broadly, it would be interesting to use this biomarker for disease diagnosis and the monitoring of the progression of the disease and the treatment effects. Moreover, since we based these findings on a mixed sample of MS participants, it would also be interesting to hone in on one type of MS longitudinally. Taken together, it would be valuable to look into perhaps different ROIs, different MRI measures and different cognitive measures.

5.3 Conclusions

Over the last few decades, with the advent and widespread availability of Magnetic Resonance Imaging (MRI) systems, brain imaging has gained an increasing role in both MS diagnosis and research[39]. Because of this, the use of more advanced quantitative methods such as DTI has revolutionized the visualization of WM structures by exploiting the properties of water diffusion[45,51]. These advanced quantitative neuroimaging techniques coupled with robust neuropsychological assessments, together, have paved the way for better understanding the structural and functional connectivity patterns in the brain. This thesis leveraged the existing knowledge in the field regarding functionally defined brain networks and the WM architecture of those networks, to support the relationship between EF and microstructure throughout the DMN and ECN WM. This thesis has showed that within this MS cohort, EF appeared to be influenced by individual differences in integrity of underlying WM throughout the DMN and ECN. These findings suggest that examination of microstructural integrity of functionally-defined WM fiber tracts can improve our understanding of the variability in cognitive functioning among persons with MS.

REFERENCES:

1. Winsen, L. M. L. Van, Polman, C. H., Dijkstra, C. D., Tilders, F. J. H. & Uitdehaag, B. M. J. Multiple Sclerosis. *Nat. Rev.* **391**, 4–7 (2010).
2. Visaria, J., Thomas, N., Gu, T., Singer, J. & Tan, H. Understanding the Patient's Journey in the Diagnosis and Treatment of Multiple Sclerosis in Clinical Practice. *Clin. Ther.* **40**, 926–939 (2018).
3. Milo, R. & Kahana, E. Multiple sclerosis: Geoepidemiology, genetics and the environment. *Autoimmun. Rev.* **9**, A387–A394 (2010).
4. Beck, C. a, Metz, L. M., Svenson, L. W. & Patten, S. B. Regional variation of multiple sclerosis prevalence in Canada. *Mult. Scler. J.* **11**, 516–519 (2005).
5. Golacre MJ, Seagroatt V, Yeates D, A. E. Linkage Study Design.Pdf. *Epidemiol. Community Heal.* **58**, 142–144 (2004).
6. T, I., WJ, G., W, C. & TM, M. Childhood sun exposure influences risk of multiple sclerosis in monozygotic twins. *Neurology* **69**, 381-- 388 8p (2007).
7. Hedström, A. K., Olsson, T. & Alfredsson, L. High body mass index before age 20 is associated with increased risk for multiple sclerosis in both men and women. *Mult. Scler. J.* **18**, 1334–1336 (2012).
8. Jakimovski, D., Guan, Y., Ramanathan, M. & Weinstock-guttman, B. Lifestyle-based modifiable risk factors in multiple sclerosis : review of experimental and clinical findings. **9**, 149–172 (2019).
9. Jakimovski, D. *et al.* Dietary and lifestyle factors in multiple sclerosis progression: results from a 5-year longitudinal MRI study. *J. Neurol.* **266**, 866–875 (2019).
10. Hedström, A. K., Hillert, J., Olsson, T. & Alfredsson, L. Smoking and multiple sclerosis

susceptibility. *Eur. J. Epidemiol.* **28**, 867–874 (2013).

11. Camara-Lemarroy, C. R., Metz, L. M. & Yong, V. W. Focus on the gut-brain axis: Multiple sclerosis, the intestinal barrier and the microbiome. *World Journal of Gastroenterology* **24**, 4217–4223 (2018).
12. Segal, B. M., Cohen, J. A. & Antel, J. Americas Committee for Treatment and Research in Multiple Sclerosis Forum 2017: Environmental factors, genetics, and epigenetics in MS susceptibility and clinical course. *Multiple Sclerosis* **24**, 4–5 (2018).
13. Munger, K. L. *et al.* Epstein–barr virus and multiple sclerosis risk in the finnish maternity cohort. *Ann. Neurol.* **86**, 436–442 (2019).
14. Yeshokumar, A., Narula, S. & Banwell, B. Pediatric multiple sclerosis. *Nevrol. Zhurnal* **22**, 64–71 (2017).
15. Hawkes, C. H. & Macgregor, A. J. Twin studies and the heritability of MS: A conclusion. *Mult. Scler.* **15**, 661–667 (2009).
16. Dyment, A. D., Sadnovich, D. & Ebers, C. G. Genetics of Multiple Sclerosis. in *Multiple Sclerosis Immunology* **6**, 197–228 (Springer New York, 2013).
17. Wingerchuk, D. M., Lucchinetti, C. F. & Noseworthy, J. H. Multiple sclerosis: Current pathophysiological concepts. *Lab. Investig.* **81**, 263–281 (2001).
18. Pröbstel, A. & Baranzini, S. E. The Role of the Gut Microbiome in Multiple Sclerosis Risk and Progression : Towards Characterization of the " MS Microbiome ". 126–134 (2018).
19. Jure, L. *et al.* Individual voxel-based analysis of brain magnetization transfer maps shows great variability of gray matter injury in the first stage of multiple sclerosis. *J. Magn. Reson. Imaging* **32**, 424–428 (2010).

20. Roman, C. A. F. & Arnett, P. A. Structural brain indices and executive functioning in multiple sclerosis: A review. *J. Clin. Exp. Neuropsychol.* **38**, 261–274 (2016).

21. Charcot, J.-M. (1825-1893). Histologie de la sclérose en plaques, leçon faite à l'hospice de la Salpêtrière par M. Charcot et recueillie par M. Bourneville. *Gaz Hop* **41**, 554–5 557–8 (1869).

22. Rocca, M. A. *et al.* Clinical and imaging assessment of cognitive dysfunction in multiple sclerosis. *Lancet Neurol.* **14**, 302–317 (2015).

23. Lassmann, H., Brück, W. & Lucchinetti, C. Heterogeneity of multiple sclerosis pathogenesis: Implications for diagnosis and therapy. *Trends Mol. Med.* **7**, 115–121 (2001).

24. Losseff, N. A. *et al.* Spinal cord atrophy and disability in multiple sclerosis. A new reproducible and sensitive MRI method with potential to monitor disease progression. *Brain* **119**, 701–708 (1996).

25. Bitsch, A. Acute axonal injury in multiple sclerosis: Correlation with demyelination and inflammation. *Brain* **123**, 1174–1183 (2002).

26. Rovira, A., Auger, C. & Alonso, J. Magnetic resonance monitoring of lesion evolution in multiple sclerosis. *Ther. Adv. Neurol. Disord.* **6**, 298–310 (2013).

27. Goverover, Y., Chiaravalloti, N. & Deluca, J. The influence of executive functions and memory on self-generation benefit in persons with multiple sclerosis. *J. Clin. Exp. Neuropsychol.* **35**, 775–783 (2013).

28. Gold, R. & Wolinsky, J. S. Pathophysiology of multiple sclerosis and the place of teriflunomide. *Acta Neurol. Scand.* **124**, 75–84 (2011).

29. Filippi, M. & Rocca, M. A. MRI evidence for multiple sclerosis as a diffuse disease of the

central nervous system. *J. Neurol.* **252**, v16–v24 (2005).

30. Mollison, D. *et al.* The clinico-radiological paradox of cognitive function and MRI burden of white matter lesions in people with multiple sclerosis: A systematic review and meta-analysis. *PLoS One* **12**, e0177727 (2017).

31. Polman, C. H. Diagnostic criteria for multiple sclerosis: 2005 Revisions to the 'McDonald criteria'. *J. Neurol.* **58**, 840–846 (2005).

32. Lublin, F. D. *et al.* Defining the clinical course of multiple sclerosis. *Neurology* **83**, 278–286 (2014).

33. Mortazavi, D., Kouzani, A. Z. & Soltanian-Zadeh, H. Segmentation of multiple sclerosis lesions in MR images: a review. *Neuroradiology* **54**, 299–320 (2012).

34. Sumowski, J. F. *et al.* Brain reserve and cognitive reserve in multiple sclerosis What you ' ve got and how you use it. *Neurology* **80**, 2186–93 (2013).

35. Sumowski, J. F., Wylie, G. R., Deluca, J. & Chiaravalloti, N. efficiency in multiple sclerosis : functional magnetic resonance imaging evidence for cognitive reserve. *J. Neurol.* **133**, 362–374 (2010).

36. Pinter, D. *et al.* Higher education moderates the effect of T2 lesion load and third ventricle width on cognition in multiple sclerosis. *PLoS One* **9**, 6–10 (2014).

37. Amato, M. P. *et al.* Cognitive reserve and cortical atrophy in multiple sclerosis A longitudinal study. 1728–1733 (2013).

38. Sumowski, J. F., Wylie, G. R., Chiaravalloti, N. & Deluca, J. Intellectual enrichment lessens the effect of brain atrophy on learning and memory in multiple sclerosis. *Neurology* **74**, 1942–1945 (2010).

39. Polman, C. H. *et al.* Diagnostic criteria for multiple sclerosis: 2010 Revisions to the

McDonald criteria. *Ann. Neurol.* **69**, 292–302 (2011).

40. Zapata-Arriaza, E. & Díaz-Sánchez, M. Clinico-radiological dissociation in multiple sclerosis: Future prospects. *World J. Neurosci.* **03**, 147–153 (2013).

41. Barkhof, F. The clinico-radiological paradox in multiple sclerosis revisited. *Curr. Opin. Neurol.* **15**, 239–245 (2002).

42. Filippi, M. *et al.* Association between pathological and MRI findings in multiple sclerosis. *Lancet Neurol.* **11**, 349–360 (2012).

43. Valverde, S. *et al.* Quantifying brain tissue volume in multiple sclerosis with automated lesion segmentation and filling. *NeuroImage Clin.* **9**, 640–647 (2015).

44. Filippi, M. MRI measures of neurodegeneration in multiple sclerosis: implications for disability, disease monitoring, and treatment. *J. Neurol.* **262**, 1–6 (2015).

45. Assaf, Y. & Pasternak, O. Diffusion Tensor Imaging (DTI)-based White Matter Mapping in Brain Research: A Review. *J. Mol. Neurosci.* **34**, 51–61 (2008).

46. Horsfield, M. A. Magnetization Transfer Imaging in Multiple Sclerosis. *J. Neuroimaging* **15**, 58S-67S (2005).

47. Prasloski, T. *et al.* Rapid whole cerebrum myelin water imaging using a 3D GRASE sequence. *Neuroimage* **63**, 533–539 (2012).

48. Rovaris, M. *et al.* Diffusion MRI in multiple sclerosis. *Neurology* **65**, 1526–1532 (2005).

49. Oreja-Guevara, C. *et al.* Progressive Gray Matter Damage in Patients With Relapsing-Remitting Multiple Sclerosis. *Arch. Neurol.* **62**, 578 (2005).

50. Roca, M. *et al.* Cognitive deficits in multiple sclerosis correlate with changes in fronto-subcortical tracts. *Multiple Sclerosis* **14**, 364–369 (2008).

51. Basser, P. J., Mattiello, J. & LeBihan, D. MR diffusion tensor spectroscopy and imaging.

Biophys. J. **66**, 259–267 (1994).

52. Horn, A. & Blankenburg, F. Toward a standardized structural–functional group connectome in MNI space. *Neuroimage* **124**, 310–322 (2016).

53. Filippi, M., Rovaris, M. & Rocca, M. A. Imaging primary progressive multiple sclerosis: the contribution of structural, metabolic, and functional MRI techniques. *Mult. Scler. J.* **10**, S36–S45 (2004).

54. Murray, T. J. Diagnosis and treatment of multiple sclerosis.

55. Thompson, A. J. *et al.* Diagnosis of multiple sclerosis: 2017 revisions of the McDonald criteria. *Lancet Neurol.* **17**, 162–173 (2018).

56. Kalkers, N. F. *et al.* Concurrent validity of the MS Functional Composite using MRI as a biological disease marker. *Neurology* **56**, 215–219 (2001).

57. Sgm, E., Liu, C. & Ld, B. Edwards(2001)Cognitive correlates of supratentorial atrophy on MRI in multiple sclerosis.pdf. 214–223 (2001).

58. Chiaravalloti, N. D. & DeLuca, J. Cognitive impairment in multiple sclerosis. *Lancet Neurol.* **7**, 1139–1151 (2008).

59. Winkelmann, A., Engel, C., Apel, A. & Zettl, U. K. Cognitive impairment in multiple sclerosis. *J. Neurol.* **254**, II35–II42 (2007).

60. Guimarães, J. & Sá, M. J. Cognitive dysfunction in Multiple Sclerosis. *Front. Neurol.* **MAY**, 1–8 (2012).

61. Bisecco, A. *et al.* Attention and processing speed performance in multiple sclerosis is mostly related to thalamic volume. *Brain Imaging Behav.* **12**, 20–28 (2018).

62. Heesen, C. *et al.* Correlates of cognitive dysfunction in multiple sclerosis. *Brain. Behav. Immun.* **24**, 1148–1155 (2010).

63. Parmenter, B. A. *et al.* Validity of the Wisconsin Card Sorting and Delis – Kaplan Executive Function System (DKEFS) Sorting Tests in multiple sclerosis. *J. Clin. Exp. neurpsychology* **29**, 215–223 (2007).

64. Arnett, P. A. *et al.* Relationship between frontal lobe lesions and Wisconsin card sorting test performance in patients with multiple sclerosis. *Neurology* **44**, 420–425 (1994).

65. Green, J. *Evaluation of General Intellectual Function, Atttention, Executive Function, Verbal Abilities, and Visuospatial and Visuoconstructive abilities*. (Academic Press, 2000).

66. Mike, A. *et al.* Identification and Clinical Impact of Multiple Sclerosis Cortical Lesions as Assessed by Routine 3T MR Imaging. 515–521 (2011). doi:10.3174/ajnr.A2340

67. Rao, S. M. *et al.* Memory Dysfunction in Multiple Sclerosis: Its Relation to Working Memory, Semantic Encoding, and Implicit Learning. *Neuropsychology* **7**, 364–374 (1993).

68. Kipps, C. M. & Hodges, J. R. Cognitive assessment for clinicians. *Neurol. Pract.* **76**, (2005).

69. Dineen, R. A. *et al.* Disconnection as a mechanism for cognitive dysfunction in multiple sclerosis. *Brain* **132**, 239–249 (2009).

70. Drew, M., Tippett, L. J., Starkey, N. J. & Isler, R. B. Executive dysfunction and cognitive impairment in a large community-based sample with Multiple Sclerosis from New Zealand: A descriptive study. *Arch. Clin. Neuropsychol.* **23**, 1–19 (2008).

71. Wuerfel, E. *et al.* Cognitive deficits including executive functioning in relation to clinical parameters in paediatric MS patients. *PLoS One* **13**, 1–15 (2018).

72. Beatty, W. W. & Monson, N. Problem Solving in Parkinson's Disease: Comparison of

Performance on the Wisconsin and California Card Sorting Tests. *J. Geriatr. Psychiatry Neurol.* **3**, 163–171 (1990).

73. Beatty, W. W., Jocic, Z., Monson, N. & Katzung, V. M. Problem Solving by Schizophrenic and Schizoaffective Patients on the Wisconsin and California Card Sorting Tests. *Neuropsychology* **8**, 49–54 (1994).

74. Genova, H. M., Deluca, J., Chiaravalloti, N. & Wylie, G. The relationship between executive functioning, processing speed, and white matter integrity in multiple sclerosis. *J. Clin. Exp. Neuropsychol.* **35**, 631–641 (2013).

75. Welton, T., Kent, D., Constantinescu, C. S., Auer, D. P. & Dineen, R. A. Functionally relevant white matter degradation in multiple sclerosis: A tract-based spatial meta-analysis. *Radiology* **275**, 89–96 (2015).

76. Uddin, L. Q., Supekar, K. S., Ryali, S. & Menon, V. Dynamic Reconfiguration of Structural and Functional Connectivity Across Core Neurocognitive Brain Networks with Development. *J. Neurosci.* **31**, 18578–18589 (2011).

77. Figley, T. D. T. D., Bhullar, N., Courtney, S. M. S. M. & Figley, C. R. C. R. Probabilistic atlases of default mode, executive control and salience network white matter tracts: an fMRI-guided diffusion tensor imaging and tractography study. *Front. Hum. Neurosci.* **9**, 1–20 (2015).

78. Buckner, R. L., Andrews-Hanna, J. R. & Schacter, D. L. The brain's default network: Anatomy, function, and relevance to disease. *Ann. N. Y. Acad. Sci.* **1124**, 1–38 (2008).

79. Seeley, W. W. *et al.* Dissociable intrinsic connectivity networks for salience processing and executive control. *J. Neurosci.* **27**, 2349–2356 (2007).

80. Filippi, M. *et al.* Association between pathological and MRI findings in multiple sclerosis.

Lancet Neurol. **11**, 349–360 (2012).

81. Assaf, Y. & Pasternak, O. Diffusion Tensor Imaging (DTI)-based White Matter Mapping in Brain Research: A Review. *J. Mol. Neurosci.* **34**, 51–61 (2008).

82. Y. Ge. Multiple Sclerosis: The Role of MR Imaging. *AJNR* **27**, 1165–1176 (2006).

83. Uddin, M. N., Figley, T. D., Marrie, R. A. & Figley, C. R. Can T 1 w/T 2 w ratio be used as a myelin-specific measure in subcortical structures? Comparisons between FSE-based T 1 w/T 2 w ratios, GRASE-based T 1 w/T 2 w ratios and multi-echo GRASE-based myelin water fractions. *NMR Biomed.* **31**, 1–11 (2018).

84. Ripollés, P. *et al.* Analysis of automated methods for spatial normalization of lesioned brains. *Neuroimage* **60**, 1296–1306 (2012).

85. Klein, A. *et al.* Evaluation of 14 nonlinear deformation algorithms applied to human brain MRI registration. *Neuroimage* **46**, 786–802 (2009).

86. Maziotta, J. C., Toga, A. W., Evans, A., Fox, P. & Lancaster, J. A probabilistic atlas of the human brain: theory and rationale for its development. *Neuroimage* **2**, 89–101 (1995).

87. Ashburner, J. & Friston, K. J. Nonlinear Spatial Normalization Using Basis Functions. *Hum. Brain Mapp.* **266**, 254–266 (1999).

88. Ashburner, J. A fast diffeomorphic image registration algorithm. *Neuroimage* **38**, 95–113 (2007).

89. Crinion, J. *et al.* Spatial normalization of lesioned brains: Performance evaluation and impact on fMRI analyses. *Neuroimage* **37**, 866–875 (2007).

90. Brett, M., Leff, A. P., Rorden, C. & Ashburner, J. Spatial Normalization of Brain Images with Focal Lesions Using Cost Function Masking. *Neuroimage* **14**, 486–500 (2001).

91. Valverde, S., Oliver, A. & Lladó, X. A white matter lesion-filling approach to improve

brain tissue volume measurements. *NeuroImage Clin.* **6**, 86–92 (2014).

92. Popescu, V. *et al.* Accurate GM atrophy quantification in MS using lesion-filling with co-registered 2D lesion masks. *NeuroImage Clin.* **4**, 366–373 (2014).

93. Battaglini, M., Jenkinson, M. & De Stefano, N. Evaluating and reducing the impact of white matter lesions on brain volume measurements. *Hum. Brain Mapp.* **33**, 2062–2071 (2012).

94. Martino, M. E. *et al.* Comparison of different methods of spatial normalization of FDG-PET brain images in the voxel-wise analysis of MCI patients and controls. *Ann. Nucl. Med.* **27**, 600–609 (2013).

95. Marrie, R. A. *et al.* Diabetes and anxiety adversely affect cognition in multiple sclerosis. *Mult. Scler. Relat. Disord.* (2019). doi:10.1016/j.msard.2018.10.018

96. Polman, C. H., Montalban, X. & Polman, C. H. Diagnostic criteria for multiple sclerosis: 2010 revisions to the McDonald criteria. *J. Neurol.* **259**, S8 (2012).

97. Kurtzke, J. F. Rating neurologic impairment in multiple sclerosis: an expanded disability status scale (EDSS). *Neurology* **33**, 1444–52 (1983).

98. Smith, S. M. Fast robust automated brain extraction. *Hum. Brain Mapp.* **17**, 143–155 (2002).

99. Acosta-Cabronero, J., Williams, G. B., Pereira, J. M. S., Pengas, G. & Nestor, P. J. The impact of skull-stripping and radio-frequency bias correction on grey-matter segmentation for voxel-based morphometry. *Neuroimage* **39**, 1654–1665 (2008).

100. Schmidt, P. *et al.* An automated tool for detection of FLAIR-hyperintense white-matter lesions in Multiple Sclerosis. *Neuroimage* **59**, 3774–3783 (2012).

101. Mori, S. *et al.* Stereotaxic white matter atlas based on diffusion tensor imaging in an

ICBM template. *Neuroimage* **40**, 570–582 (2008).

102. Beg, M. F., Miller, M. I., Trou, A. & Younes, L. Computing Large Deformation Metric Mappings via Geodesic Flows of Diffeomorphisms. *Int. J. Comput. Vis.* **61**, 139–157 (2005).

103. Jenkinson, M. & Smith, S. A global optimisation method for robust affine registration of brain images. *Med. Image Anal.* **5**, 143–156 (2001).

104. Jenkinson, M., Bannister, P., Brady, M. & Smith, S. Improved Optimization for the Robust and Accurate Linear Registration and Motion Correction of Brain Images. *Neuroimage* **17**, 825–841 (2002).

105. Andersson, J. L. R., Jenkinson, M., Smith, S. & Andersson, J. *FNIRT — FMRIB' non-linear image registration tool*. *Oxford Centre for Functional Magnetic Resonance imaging of the Brain, Department of Clinical Neurology, Oxford University, Oxford, UK* (2007).

106. Avants, Brian B. Tustiscon, Nick. Song, G. Advanced Normalization Tools (ANTS). (2011).

107. Gaser, Christian, D. R. CAT - A computational anatomy toolbox for the analysis of structural MRI data. 336–348 (2016).

108. Ashburner, J. & Friston, K. J. Diffeomorphic registration using geodesic shooting and Gauss–Newton optimisation. *Neuroimage* **55**, 954–967 (2011).

109. Kvålseth, T. On Normalized Mutual Information: Measure Derivations and Properties. *Entropy* **19**, 631 (2017).

110. González-Villà, S., Oliver, A., Huo, Y., Lladó, X. & Landman, B. A. Brain structure segmentation in the presence of multiple sclerosis lesions. *NeuroImage Clin.* **22**, 101709

(2019).

111. Oishi, K. *et al.* Atlas-based whole brain white matter analysis using large deformation diffeomorphic metric mapping: Application to normal elderly and Alzheimer's disease participants. *Neuroimage* **46**, 486–499 (2009).

112. Dice, L. Measures of the amount of ecological association between species. *Ecology* **26**, 297–302 (1945).

113. Zou, K. H. *et al.* Statistical Validation of Image Segmentation Quality Based on a Spatial Overlap Index 1 : Scientific Reports. *Acad Radiol* **11**, 178–189 (2004).

114. Kutzelnigg, A. *et al.* Cortical demyelination and diffuse white matter injury in multiple sclerosis. *Brain* **128**, 2705–2712 (2005).

115. Shu, N. *et al.* Diffusion tensor tractography reveals disrupted topological efficiency in white matter structural networks in multiple sclerosis. *Cereb. Cortex* **21**, 2565–2577 (2011).

116. Trenova, A. G. *et al.* Cognitive Impairment in Multiple Sclerosis. *Folia Med. (Plovdiv).* **58**, (2016).

117. Llufriu, S. *et al.* Structural networks involved in attention and executive functions in multiple sclerosis. *NeuroImage Clin.* **13**, 288–296 (2017).

118. Drew, M. A., Starkey, N. J. & Isler, R. B. Examining the link between information processing speed and executive functioning in multiple sclerosis. *Arch. Clin. Neuropsychol.* **24**, 47–58 (2009).

119. Mattioli, F., Stampatori, C., Bellomi, F., Scarpazza, C. & Galli, P. Assessing executive function with the D-KEFS sorting test : normative data for a sample of the Italian adult population. 1895–1902 (2014). doi:10.1007/s10072-014-1857-7

120. Jefferson, A. L., Paul, R. H., Ozonoff, A. & Cohen, R. A. Evaluating elements of executive functioning as predictors of instrumental activities of daily living (IADLs). *Arch. Clin. Neuropsychol.* **21**, 311–320 (2006).

121. Smith, E. E. *et al.* Correlations between MRI white matter lesion location and executive function and episodic memory. *Neurology* **76**, 1492–1499 (2011).

122. Davis, F. A. The clinico-radiological paradox in multiple sclerosis: novel implications of lesion size. *Mult. Scler. J.* **20**, 515–516 (2014).

123. Artemiadis, A., Anagnostouli, M., Zalonis, I., Chairopoulos, K. & Triantafyllou, N. Structural MRI correlates of cognitive function in multiple sclerosis. *Mult. Scler. Relat. Disord.* **21**, 1–8 (2018).

124. Eijlers, A. J. C. *et al.* Predicting cognitive decline in multiple sclerosis: A 5-year follow-up study. *Brain* **141**, 2605–2618 (2018).

125. Hawellek, D. J., Hipp, J. F., Lewis, C. M., Corbetta, M. & Engel, A. K. Increased functional connectivity indicates the severity of cognitive impairment in multiple sclerosis. *Proc. Natl. Acad. Sci. U. S. A.* **108**, 19066–19071 (2011).

126. Tahedl, M., Levine, S. M., Greenlee, M. W., Weissert, R. & Schwarzbach, J. V. Functional connectivity in multiple sclerosis: Recent findings and future directions. *Front. Neurol.* **9**, 1–18 (2018).

127. Eshaghi, A. *et al.* Classification algorithms with multi-modal data fusion could accurately distinguish neuromyelitis optica from multiple sclerosis. *NeuroImage Clin.* **7**, 306–314 (2015).

128. Figley, C. R., Asem, J. S. A., Levenbaum, E. L. & Courtney, S. M. Effects of Body Mass Index and Body Fat Percent on Default Mode , Executive Control , and Salience Network

Structure and Function. **10**, 1–23 (2016).

129. Dimitrov, M., Grafman, J., Soares, A. H. R. & Clark, K. Concept formation and concept shifting in frontal lesion and Parkinson's disease patients assessed with the California card sorting test. *Neuropsychology* **13**, 135–143 (1999).

130. Crouch, J. A., Greve, K. W. & Brooks, J. The California Card Sorting Test may dissociate verbal and non-verbal concept formation abilities. *Br. J. Clin. Psychol.* **35**, 431–434 (1996).

131. Delis, D. C., Squire, L. R., Bihrle, A. & Massman, P. Componential analysis of problem-solving ability: Performance of patients with frontal lobe damage and amnesic patients on a new sorting test. *Neuropsychologia* **30**, 683–697 (1992).

132. Berg, J. L., Swan, N. M., Banks, S. J. & Miller, J. B. Atypical performance patterns on Delis–Kaplan Executive Functioning System Color–Word Interference Test: Cognitive switching and learning ability in older adults. *J. Clin. Exp. Neuropsychol.* **38**, 745–751 (2016).

133. Till, C. *et al.* Magnetic resonance imaging predictors of executive functioning in patients with pediatric-onset multiple sclerosis. *Arch. Clin. Neuropsychol.* **27**, 495–509 (2012).

134. Caruyer, E., Aganj, I., Lenglet, C., Sapiro, G. & Deriche, R. Motion detection in diffusion MRI via online ODF estimation. *Int. J. Biomed. Imaging* **2013**, (2013).

135. Sotiropoulos, S. N. *et al.* Advances in diffusion MRI acquisition and processing in the Human Connectome Project. *Neuroimage* **80**, 125–143 (2013).

136. Uğurbil, K. *et al.* Pushing spatial and temporal resolution for functional and diffusion MRI in the Human Connectome Project. *Neuroimage* **80**, 80–104 (2013).

137. Mohammadi, S., Möller, H. E., Kugel, H., Müller, D. K. & Deppe, M. Correcting eddy

current and motion effects by affine whole-brain registrations: Evaluation of three-dimensional distortions and comparison with slicewise correction. *Magn. Reson. Med.* **64**, 1047–1056 (2010).

138. Ruthotto, L. *et al.* Diffeomorphic susceptibility artifact correction of diffusion-weighted magnetic resonance images. *Phys. Med. Biol.* **57**, 5715–5731 (2012).

139. Mohammadi, S., Freund, P., Feiweier, T., Curt, A. & Weiskopf, N. The impact of post-processing on spinal cord diffusion tensor imaging. *Neuroimage* **70**, 377–385 (2013).

140. Meng, X.-L., Rosenthal, R. & Rubrin, D. Comparing Correlated Correlation Coefficients. *Quant. methods Psychol.* **111**, 172–175 (1992).

141. Diedenhofen, B. & Musch, J. Cocor: A comprehensive solution for the statistical comparison of correlations. *PLoS One* **10**, 1–12 (2015).

142. Cruz-Gómez, Á. J., Ventura-Campos, N., Belenguer, A., Ávila, C. & Forn, C. The link between resting-state functional connectivity and cognition in MS patients. *Mult. Scler. J.* **20**, 338–348 (2014).

143. Roosendaal, S. D. *et al.* Resting state networks change in clinically isolated syndrome. *Brain* **133**, 1612–1621 (2010).

144. Bonavita, S. *et al.* Distributed changes in default-mode resting-state connectivity in multiple sclerosis. *Mult. Scler. J.* **17**, 411–422 (2011).

145. Sacco, R., Bonavita, S., Esposito, F., Tedeschi, G. & Gallo, A. The Contribution of Resting State Networks to the Study of Cortical Reorganization in MS. *Mult. Scler. Int.* **2013**, 1–7 (2013).

146. Rocca, M. A. *et al.* Default-mode network dysfunction and cognitive impairment in progressive MS. *Neurology* **74**, 1252–1259 (2010).

147. Daselaar, S. M. *et al.* Less wiring, more firing: Low-performing older adults compensate for impaired white matter with greater neural activity. *Cereb. Cortex* **25**, 983–990 (2015).

148. Bodini, B. *et al.* Exploring the relationship between white matter and gray matter damage in early primary progressive multiple sclerosis: An in vivo study with TBSS and VBM. *Hum. Brain Mapp.* **30**, 2852–2861 (2009).

149. Solana, E. *et al.* Modified connectivity of vulnerable brain nodes in multiple sclerosis , their impact on cognition and their discriminative value. *Sci. Rep.* **9**, 1–8 (2019).

150. Savini, G. *et al.* Default mode network structural integrity and cerebellar connectivity predict information processing speed deficit in multiple sclerosis. *Front. Cell. Neurosci.* **13**, 1–15 (2019).

151. Denney, D. R. & Lynch, S. G. The impact of multiple sclerosis on patients' performance on the Stroop Test: Processing speed versus interference. *J. Int. Neuropsychol. Soc.* **15**, 451–458 (2009).

152. Yu, H. J. *et al.* Multiple white matter tract abnormalities underlie cognitive impairment in RRMS. *Neuroimage* **59**, 3713–3722 (2012).

153. Tovar-Moll, F. *et al.* Thalamic involvement and its impact on clinical disability in patients with multiple sclerosis: A diffusion tensor imaging study at 3T. *Am. J. Neuroradiol.* **30**, 1380–1386 (2009).

154. Benedict, Ralph HB, Bruce, Jared, G Dwyer Michael, Weinstock-Guttman, Bianca, Tjoa, Chris, Tavazza, Eleonora, Munschauer, Frederick E, Zivadinov, R. Diffusion-weighted imaging predicts cognitive impairment in multiple sclerosis.pdf. *Mult. Scler.* **13**, 722–730 (2007).

155. Klein, A. *et al.* Evaluation of 14 nonlinear deformation algorithms applied to human brain

MRI registration. *Neuroimage* **46**, 786–802 (2009).

156. Ripollés, P. *et al.* Analysis of automated methods for spatial normalization of lesioned brains. *Neuroimage* **60**, 1296–1306 (2012).

157. Martino, M. E. *et al.* Comparison of different methods of spatial normalization of FDG-PET brain images in the voxel-wise analysis of MCI patients and controls. *Ann. Nucl. Med.* **27**, 600–609 (2013).